NAVY DEPARTMENT

THE DAVID W. TAYLOR MODEL BASIN

WASHINGTON 7, D.C.

EXPLORATORY INVESTIGATION OF THE TURBULENT WAKES BEHIND BLUFF BODIES

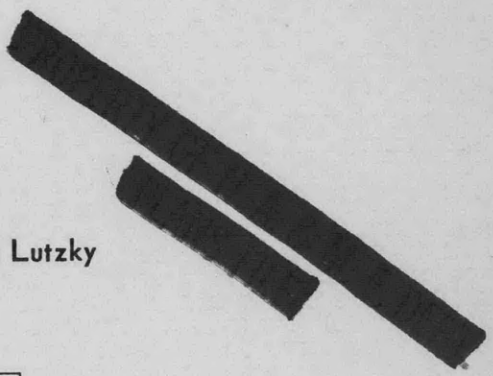

by

Ralph D. Cooper and Morton Lutzky

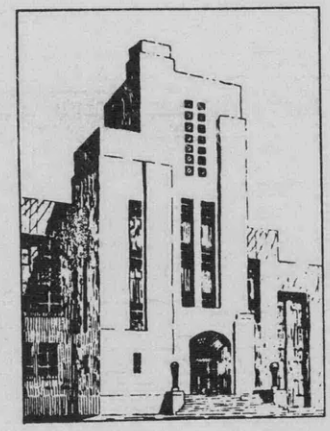

RESEARCH AND DEVELOPMENT REPORT

October 1955

Report 963

EXPLORATORY INVESTIGATION OF THE TURBULENT WAKES BEHIND BLUFF BODIES

by

Ralph D. Cooper and Morton Lutzky

October 1955

Report 963
NS715-102

TABLE OF CONTENTS

	Page
ABSTRACT	1
INTRODUCTION	1
THEORETICAL CONSIDERATIONS	2
APPARATUS AND PROCEDURES	5
RESULTS AND DISCUSSION	7
Basic Data	7
Similarity Analysis	13
CONCLUSIONS	22
APPENDIX A - THE REYNOLDS EQUATIONS OF MOTION AND THE ENERGY EQUATION OF TURBULENCE	23
Derivation	23
Expansion into Cylindrical Coordinates	24
Simplification in the Case of Axial Symmetry	25
APPENDIX B - DERIVATION OF APPROXIMATE EQUATIONS OF FLUID MOTION	27
REFERENCES	29

NOTATION

A_w	Cross-sectional area of the wake
b	Width of plate
D	Total drag
d	Diameter of circular disc
f, g, h, j	Universal functions of η appearing in similarity relations
r_0	Radius of the mean wake behind circular disc
$(r_{1/2})_f$	Radius of fluctuating wake behind disc at which $u' = \frac{1}{2}(u')_{max}$
$(r_{1/2})_m$	Radius of mean wake behind disc at which $U_d = \frac{1}{2}(U_d)_{max}$
t	Time
U, V, W	Mean velocity components in the x, r, and θ directions respectively
U_d	Mean velocity defect ($= U_0 - U$)
U_0	Free stream velocity
u, v, w	Fluctuating velocity components in the x, r, and θ directions respectively
u'	$\sqrt{\overline{u^2}} = \left[\lim_{T\to\infty} \frac{1}{T}\int_{-T/2}^{T/2} u^2\, dt\right]^{1/2}$ = root-mean-square value of u
x, r, θ	Cylindrical coordinates
$(z_{1/2})_f$	Width of fluctuating wake behind plate at which $u' = \frac{1}{2}(u')_{max}$
$(z_{1/2})_m$	Width of mean wake behind plate at which $U_d = \frac{1}{2}(U_d)_{max}$
α, β	Exponents appearing in similarity relations
ρ	Density of fluid
$\eta = \frac{r}{x^\beta}$	New independent variable
λ	Microscale of turbulence
ν	Kinematic viscosity
Φ	Dissipation function

Note: The bar is used to indicate the mean value of fluctuating quantities.

ABSTRACT

The mean velocity and the turbulence intensity of the axial component of the fluctuating velocity were measured in the wakes behind a disc and a series of four rectangular plates.

For axially symmetric wakes, in agreement with theoretical results derived from similarity considerations, it was found that

1. the maximum values of the mean velocity defect U_d and the turbulence intensity u' vary inversely as $x^{2/3}$ where x denotes the axial position in the wake;

2. the radius of the wake varies as $x^{1/3}$;

3. transverse distributions of U_d and u' are universal functions of $\eta = r/x^{1/3}$, where r denotes the radial position in the wake.

The microscale of turbulence λ was found experimentally to vary as $x^{1/4}$ in contrast to the $x^{1/2}$ variation theoretically predicted from similarity considerations.

INTRODUCTION

The Reynolds numbers associated with most practical problems involving the flow of fluids are, in general, so large that the resultant fluid motion is turbulent. In accordance with a hypothesis introduced by O. Reynolds,[1] such a motion is assumed to be separable into a mean motion, which at most varies slowly with respect to time, and a superposed fluctuating motion, which by comparison varies very rapidly with time. The latter motion is further characterized by velocity components whose temporal averages vanish identically.

Current concepts of some of the highly complex processes involved in turbulent flow stem directly from appropriate application of this classical description of turbulence to the Navier-Stokes equations of motion. Processes such as the transfer of energy from the mean to the fluctuating motion and the dissipation of energy to heat by the direct action of viscosity are illustrative of the complicated interrelationships encountered in the phenomenon of turbulence.

Notable among investigations concerned with the decay of energy in turbulent flows are those that have been conducted in the flow behind screens and grids,[2, 3] in jet flow,[4, 5] and in the wake behind a two-dimensional circular cylinder.[6, 7]

This report gives the results of an experimental investigation of the turbulent wakes behind a circular disc and a series of rectangular plates mounted normal to a steady, uniform air stream. Interest in the investigation is focused primarily on the axial variation of such

---

[1] References are listed on pages 29-30.

characteristic quantities of wake flows as the turbulence intensity, the mean velocity defect, the microscale of turbulence, and the dimension of the wake.

THEORETICAL CONSIDERATIONS

Problems dealing with turbulent flows are, in general, formulated in accordance with the so-called Reynolds equations of motion, which result from introducing into the Navier-Stokes equations the concept of separable mean and fluctuating components of the motion. (A detailed derivation of the Reynolds equations is given in Appendix A.) Unfortunately, in almost all cases these equations are intractable to present mathematical techniques. As a consequence, the Reynolds equations sufficiently far downstream from the origin of a turbulent wake are customarily simplified by introducing the usual boundary layer type assumptions that (1) the pressure gradient in the direction of the mean motion is negligible, (2) the viscous effects are small in comparison to those due to the so-called Reynolds stresses, and (3) the gradient of these stresses in the direction of the mean motion is small in comparison to their gradients in the transverse directions.

Under these assumptions, a first approximation to the case of an axially symmetric turbulent wake can be obtained from the Reynolds equations of motion by neglecting second order terms in the mean velocity components and their derivatives, viz.,

$$U_0 \frac{\partial U_d}{\partial x} = \frac{1}{r} \frac{\partial}{\partial r} r \overline{uv} \qquad [1]$$

where U_0 is the free stream velocity,

U_d is the so-called mean velocity defect defined as the difference $U_0 - U$,

U is the mean velocity component in the axial direction,

$\overline{uv}$ is a Reynolds shear stress defined as the temporal average of the instantaneous product of the axial velocity component u and the radial velocity component v of the fluctuating motion, and

x, r are the axial and radial components of a cylindrical coordinate system.

(A more rigorous derivation of this simplified equation is given in Appendix B.)

From Equation [1] it appears most probable that an independent relation between the mean velocity defect and the Reynolds shear stress would resolve the difficulties associated with this equation and permit its analytical solution. Attempts to bridge the gap occasioned by the lack of such a relation led to the evolution of the so-called mixing length theories, e.g., the momentum transfer theory of L. Prandtl[8] and the vorticity transfer theory of G.I. Taylor,[9] which although moderately successful in describing the mean flow gave virtually no information whatsoever concerning the fluctuating flow.

However, several important aspects of axially symmetric turbulent wakes can be simply deduced from Equation [1] by application of the similarity principles of Th. von Kármán.[10]

Basically, the theory of similarity hypothesizes that sufficiently far downstream in the wake the flow processes have achieved a state of statistical equilibrium such that transverse distributions of a significant flow parameter at various stations are self-preserving in the sense that they can be made universal by suitable adjustments of their magnitude and length scales with factors which are functions of the axial position only. In particular, similarity solutions for which these adjusting factors are simply monomials in x are sought; generally, monomials of nonintegral degree are encountered, and the degree of the factor associated with the magnitude scale is not necessarily the same as that associated with the length scale.

In the axially symmetric case under investigation here, these similarity considerations lead to the condition that relations of the form

$$\frac{U_d}{U_0} = \frac{f(\eta)}{x^\alpha}, \quad \frac{\overline{uv}}{U_0^2} = \frac{g(\eta)}{x^{2\alpha}}, \quad \eta = \frac{r}{x^\beta} \qquad [2]$$

be found such that their introduction into [1] results in an equation whose individual terms are all of the same order in x; in other words, similarity considerations require that suitable transformations of both the independent and dependent variables be found such that the simplified Reynolds equation is reduced to an ordinary differential equation in the new variable η. As is easily verified by inserting [2] into [1], this condition is satisfied for

$$\alpha + \beta = 1 \qquad [3]$$

An additional relation between the exponents α and β is imposed by the condition that the drag D of the body creating the wake is equal to the total momentum loss suffered by the fluid in flowing past the body. This condition in the axially symmetric case can be expressed mathematically as an integral across the wake at an arbitrary downstream position, viz.,

$$D = \iint_{A_w} \rho\, U (U_0 - U)\, dA_w \approx 2\pi\, \rho\, U_0 \int_0^{r_0} U_d\, r dr \qquad [4]$$

where A_w is the cross-sectional area of the wake at any axial station and r_0 is the associated radius which, of course, denotes the edge of the wake, i.e., $U_d(r_0) = 0$. It is important to note that the approximate form of the momentum loss integral given above is consistent with the approximate form of the equation of motion [1].

For the present purposes, the most significant aspect of [4] is the condition that the integral is required to be independent of x, since the drag itself, of course, exhibits no such dependency. The insertion of [2] into [4] readily demonstrates that this condition is satisfied for

$$\alpha = 2\beta \qquad [5]$$

Relations [3] and [5] then permit a unique specification of the similarity solution proposed in [2] such that

$$\alpha = \frac{2}{3}, \quad \beta = \frac{1}{3}$$

Now, with the further assumption that in the case under consideration all elements of the Reynolds stress tensor behave in a manner analogous to the element $\overline{uv}$, i.e., in particular that

$$\frac{\overline{u^2}}{\overline{uv}} = h(\eta)$$

the results of the application of similarity considerations to the simplified equation of motion of an axially symmetric turbulent wake may be summarized as follows:

1. The maximum value of the mean velocity defect U_d varies inversely as $x^{2/3}$.

2. The maximum value of the turbulence intensity component u' (the prime denotes the root-mean-square value of u) varies inversely as $x^{2/3}$.

3. The radius of the wake r_0 varies as $x^{1/3}$.

4. Transverse distributions of U_d and u' are universal functions of $\eta = r/x^{1/3}$.

The equivalent characteristic behavior of the microscale of turbulence λ can be investigated with the aid of the so-called energy equation of turbulence, whose derivation is given in Appendix A. As shown in Appendix B, the simplification of this equation in the case of the axially symmetric turbulent wake presently under consideration to a first order approximation consistent with Equation [1] results in

$$U_0 \frac{\partial}{\partial x} \frac{\overline{u^2} + \overline{v^2} + \overline{w^2}}{2} = \overline{uv} \frac{\partial U_d}{\partial r} - \nu \Phi \qquad [6]$$

where Φ is the dissipation function and is indicative of the energy of the fluctuating motion converted to heat by the direct action of viscosity. The left-hand side of Equation [6] can be related physically to the convection of energy of the fluctuating motion by the mean flow; the first term on the right-hand side is a measure of the energy transfer from the mean motion to the fluctuating motion.

In order to apply the similarity relations, previously determined from consideration of the simplified equation of motion, to the energy equation [6], it is convenient to introduce an expression for the dissipation function that is more amenable to analysis than its exact representation. To this end, Φ is assumed to be satisfactorily described by its representation in the case of isotropic turbulence, viz.,

$$\Phi = 15 \frac{\overline{u^2}}{\lambda^2} \qquad [7]$$

Application of the previous results relating to the functional forms of the mean velocity defect and Reynolds stress tensor elements indicates that similarity conditions are satisfied by the energy equation [6] when the dissipation function has its isotropic form [7] if

$$\lambda = x^{1/2} j(\eta)$$

It is of interest to note that this variation of λ with x is consistent with that obtained in the case of isotropic turbulence when a simple power-law dependence of the energy on the independent variable is postulated.

In a subsequent portion of this paper, the theoretical results determined here by means of similarity considerations will be compared with experimental results.

APPARATUS AND PROCEDURES

The experiments were conducted in the TMB Low Turbulence Wind Tunnel. This tunnel is of the open-return type and has a test section 4 feet high, 2 feet wide, and 14.5 feet long. (Actually, the test section side walls are flexible and the width specified here corresponds to the unflexed or parallel wall position.) The air speed in the test section is continuously variable from approximately 20 fps to 150 fps. The low background turbulence level of the test section air stream, which is of the order of 0.1 percent, is obtained primarily through the use of a set of six turbulence damping screens installed upstream of the 12.5:1 contraction cone.

The test configurations consist of a circular disc and a series of four rectangular plates with aspect ratios of 1, 3, 5, and 10, respectively. Each of the configurations is made of brass, is 0.03 inch thick, and has a diameter d or width b, as appropriate, of 0.2 inch. They were mounted normal to the air flow at a position approximately on the tunnel axis near the upstream end of the test section by means of two very fine support wires. The diameter of these support wires is 0.001 inch in the case of the disc and the two smaller plates and 0.004 inch in the case of the two larger plates. The plates were oriented in the test section with their long sides vertical.

At five stations in the wake, measurements of the transverse distribution of the mean velocity U and the turbulence intensity of the axial component of the fluctuating velocity u' were made at elevations corresponding to the plane of horizontal symmetry of the configurations; in addition, the microscale of turbulence λ was measured at the transverse position corresponding to maximum turbulence intensity. The measuring stations, which vary slightly with each installation, extend from approximately 15 to 680 disc diameters or plate widths downstream of the configurations. Figure 1 is a schematic diagram of the wind tunnel test section illustrating the coordinate system, the position of the test configuration and the orientation of a typical turbulence level distribution.

For reasons associated with the facility and dependability with which the data could be obtained, the majority of the u' measurements were made at a free stream speed U_0 of 80 fps, and the U measurements were made exclusively at U_0 = 140 fps. Exceptions to this condition on the stream speed at which turbulence was measured occurred only in the case of the disc, in which case u' was measured at the additional speeds U_0 = 35 and 140 fps. The disc also constitutes the only configuration for which no mean flow measurements were made. Based on disc diameters or plate widths, the Reynolds numbers corresponding to U_0 = 35, 80, and 140 fps are 3600, 8300, and 14,500, respectively.

The free stream velocity in the test section was measured with conventional total head and static pressure probes used in conjunction with a slanted, multitube, alcohol-filled manometer system.

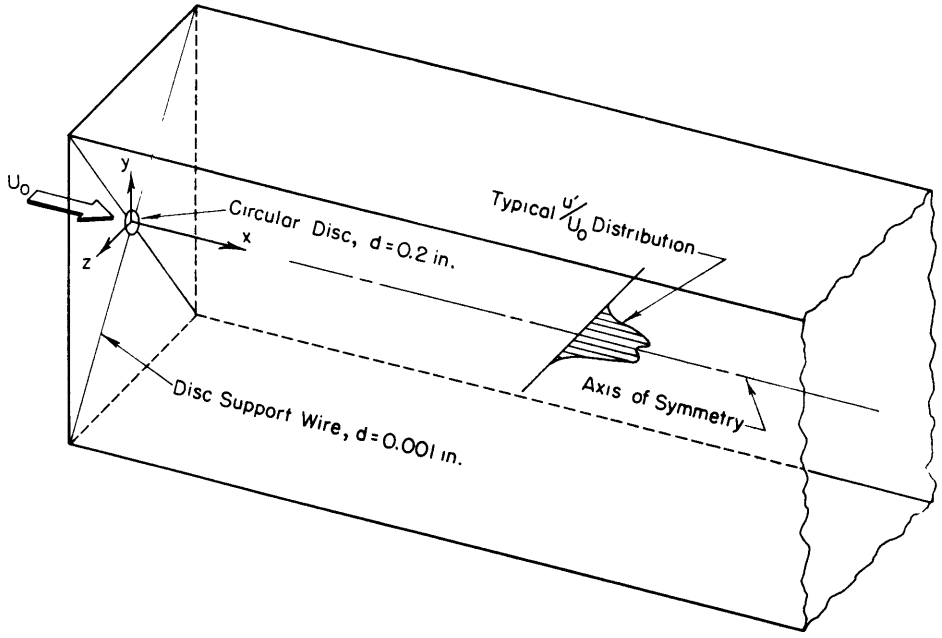

Figure 1 - Schematic Diagram of Wind Tunnel Test Section Illustrating the Coordinate System, the Position of the Disc, and a Typical Turbulence Level Distribution

The mean velocity at a point in the wake was determined from measurement of the total head at the point under the assumption that the static pressure, which was independently measured to determine the free stream velocity, is constant throughout any transverse plane across the test section. The estimated error in mean velocity measurement as a result of the moderately intense turbulence field is negligibly small and no correction was made for it.

The turbulence measurements were made with a constant temperature hot-wire anemometer constructed for the Taylor Model Basin by the Iowa Institute of Hydraulic Research. A timewise differentiating circuit incorporated in the anemometer permits the calculation of the microscale from the relation

$$\frac{1}{\lambda^2} = \frac{1}{\overline{u^2}}\overline{\left(\frac{\partial u}{\partial x}\right)^2} \approx \frac{1}{U^2\overline{u^2}}\overline{\left(\frac{\partial u}{\partial t}\right)^2}$$

where the bar indicates a temporal average. The sensing element of the hot-wire probe is a tungsten wire which has a diameter of 0.00014 inch and an active length of about 0.025 inch. To obtain a signal proportional to the u-component of the fluctuating velocity, the axis of this element must, of course, be oriented normal to the mean flow. Based on the assumptions that the energies of two uncorrelated, superposed turbulent fields combine linearly and that the background level of turbulence remains constant throughout the wake, the measured turbulence intensities were corrected in accordance with the following relation:

$$\overline{u^2}_{\text{corrected}} = \overline{u^2}_{\text{measured}} - \overline{u^2}_{\text{background}}$$

It should be noted that, in general, this correction was negligibly small with reference to the maximum value of a particular distribution; its effect, of course, increased as the edge of the wake was approached.

Transverse traverses of the turbulent wake were made by means of a mechanism, mounted in the test section but externally controlled, which accommodates either the hot-wire probe for turbulence measurements or the total head tube for mean flow measurements.

Figure 2 is a photograph looking downstream, that shows the hot-wire probe, the traversing mechanism, and the reference total head and static pressure probes installed in the test section of the wind tunnel.

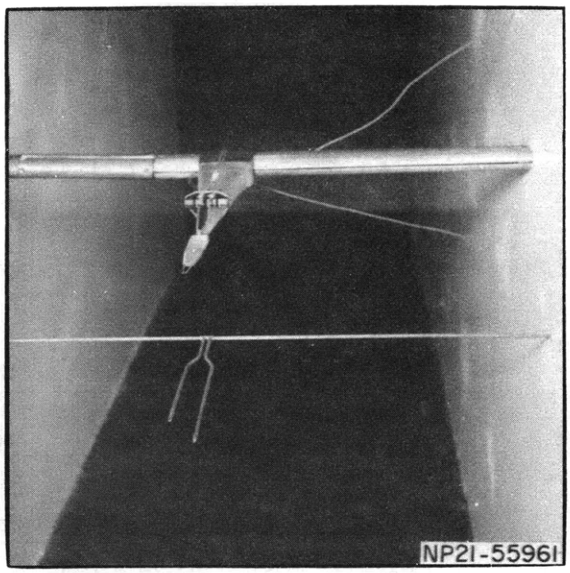

Figure 2 - Downstream View of the Hot-Wire Probe, the Traversing Mechanism, and the Reference Total Head and Static Pressure Probe

RESULTS AND DISCUSSION

BASIC DATA

The radial distributions of u'/U_0 at the various measuring stations in the wake behind the circular disc are shown in Figure 3 as a function of the nondimensionalized radial coordinate $r/(d/2)$ for three conditions of the free stream velocity U_0 = 35, 80, 140 fps. (Measurements at the highest speed were curtailed because of instrumentation limitations resulting from high anemometer signal-to-noise ratios at the more remote stations.) As comparison of these data indicated no marked Reynolds number effect on the magnitude of the maximum turbulence intensity, all subsequent turbulence measurements were made at $U_0 = 80$ fps.

In Figures 4 to 7, the transverse distributions of u'/U_0 and U_d/U_0 at the various measuring stations in the wake behind the four rectangular plates are shown as a function of the nondimensionalized transverse spatial coordinate $z/(b/2)$.

As in the case of the disc, an off-center maximum in the turbulence intensity distribution occurs at every station behind each plate; the general shapes of the u'/U_0 distributions at equivalent x/b stations are very similar for all configurations. On the other hand, the mean velocity defect distributions for all plates except the first show a marked off-center maximum at the initial measuring stations, which becomes more pronounced as the aspect ratio of the test configuration increases. As they progress downstream, these distributions slowly change to the more conventional wake profiles characterized by a maximum velocity defect at the plane of symmetry, as exhibited in the distributions at all stations behind Plate I.

(Text continued on page 13.)

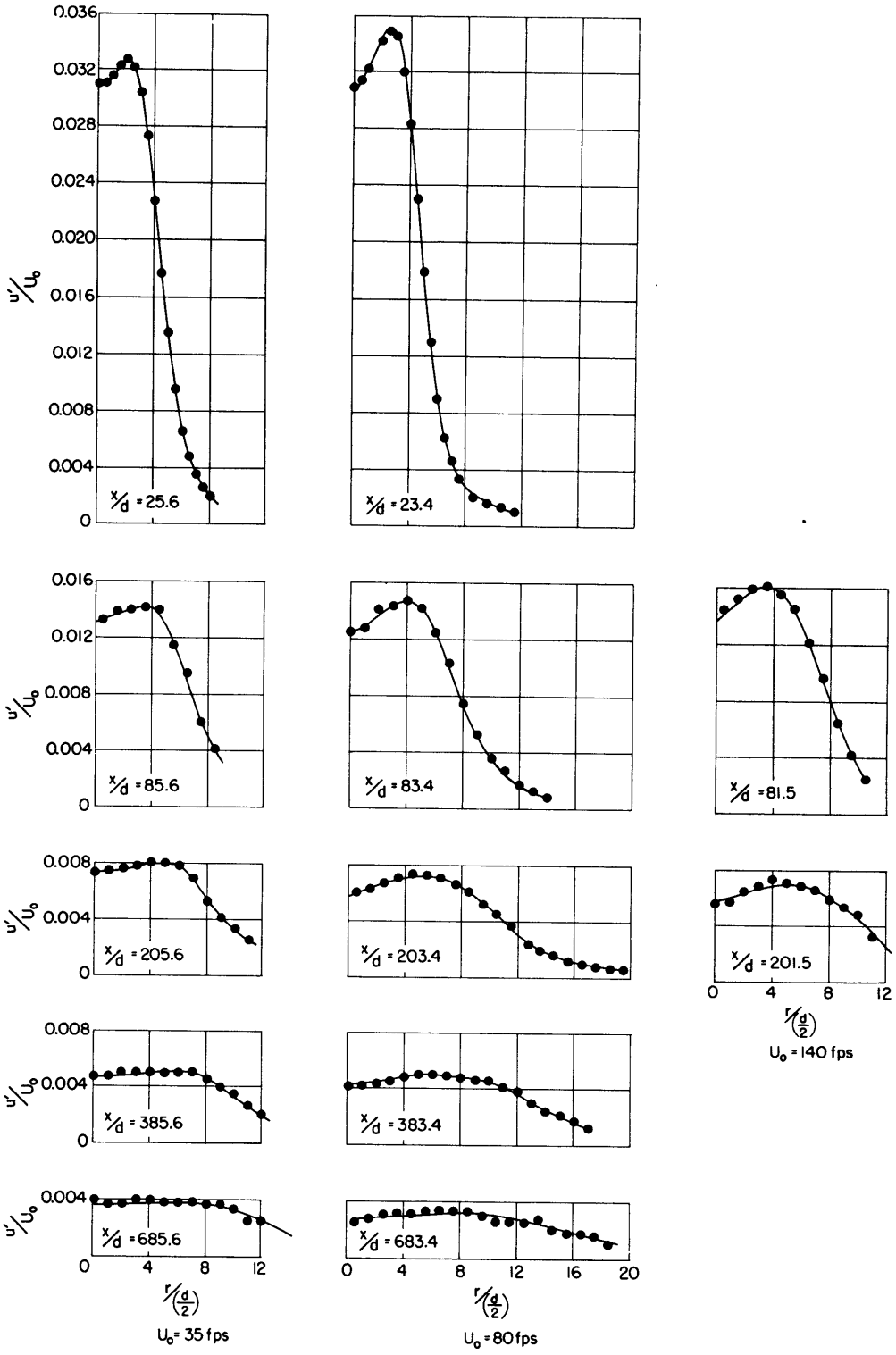

Figure 3 - Radial Distributions of the Intensity of the Axial Component of the Turbulent Velocity in the Wake behind a Disc (d = 0.2 Inch)

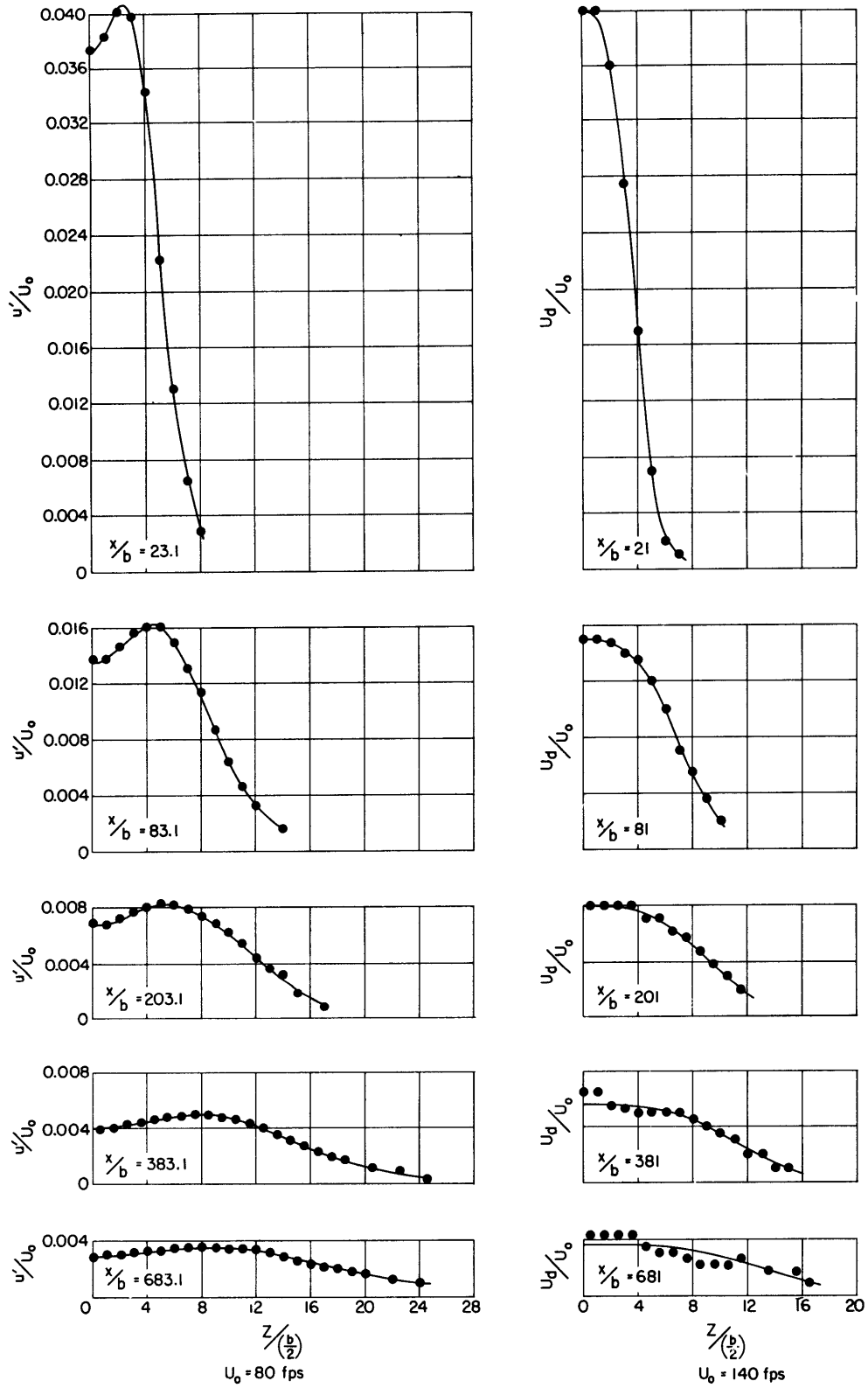

Figure 4 - Transverse Distributions of the Longitudinal Component of the Turbulent and Mean Velocity in the Wake behind Plate I (l/b = 1, b = 0.2 Inch)

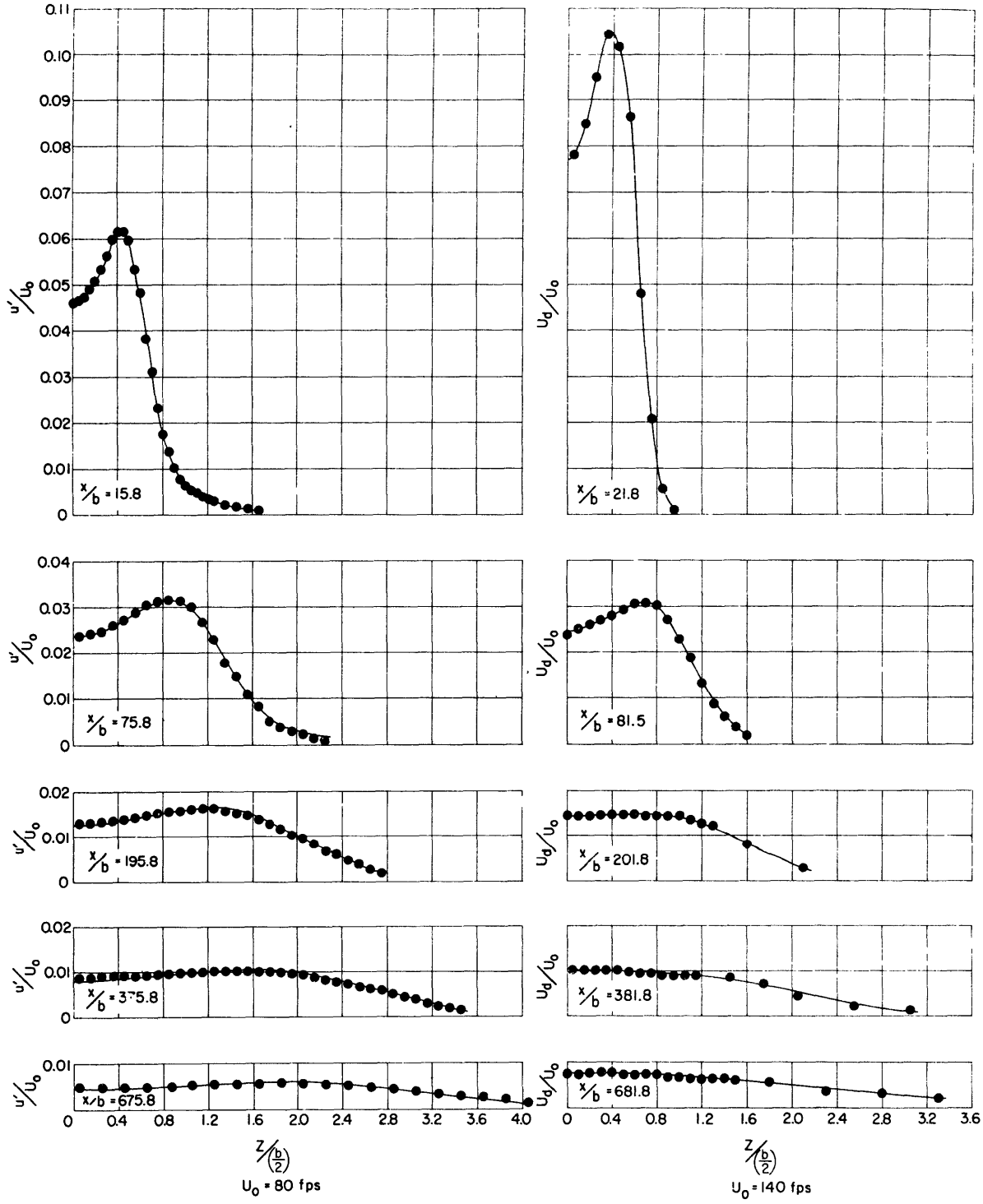

Figure 5 - Transverse Distributions of the Longitudinal Component of the Turbulent and Mean Velocity in the Wake behind Plate II (l/b = 3, b = 0.2 Inch)

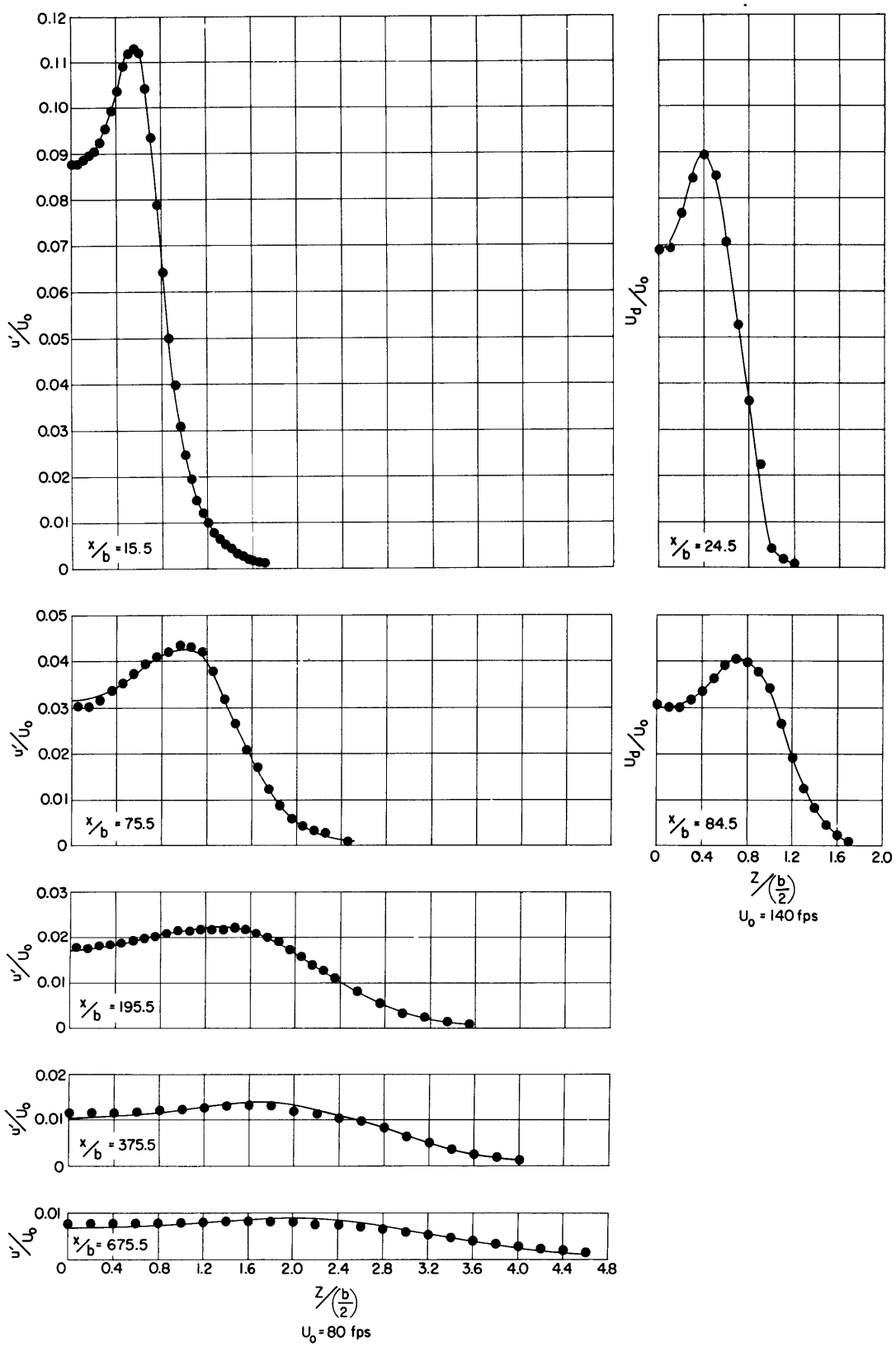

Figure 6 - Transverse Distributions of the Longitudinal Component of the Turbulent and Mean Velocity in the Wake behind Plate III ($l/b = 5$, $b = 0.2$ Inch)

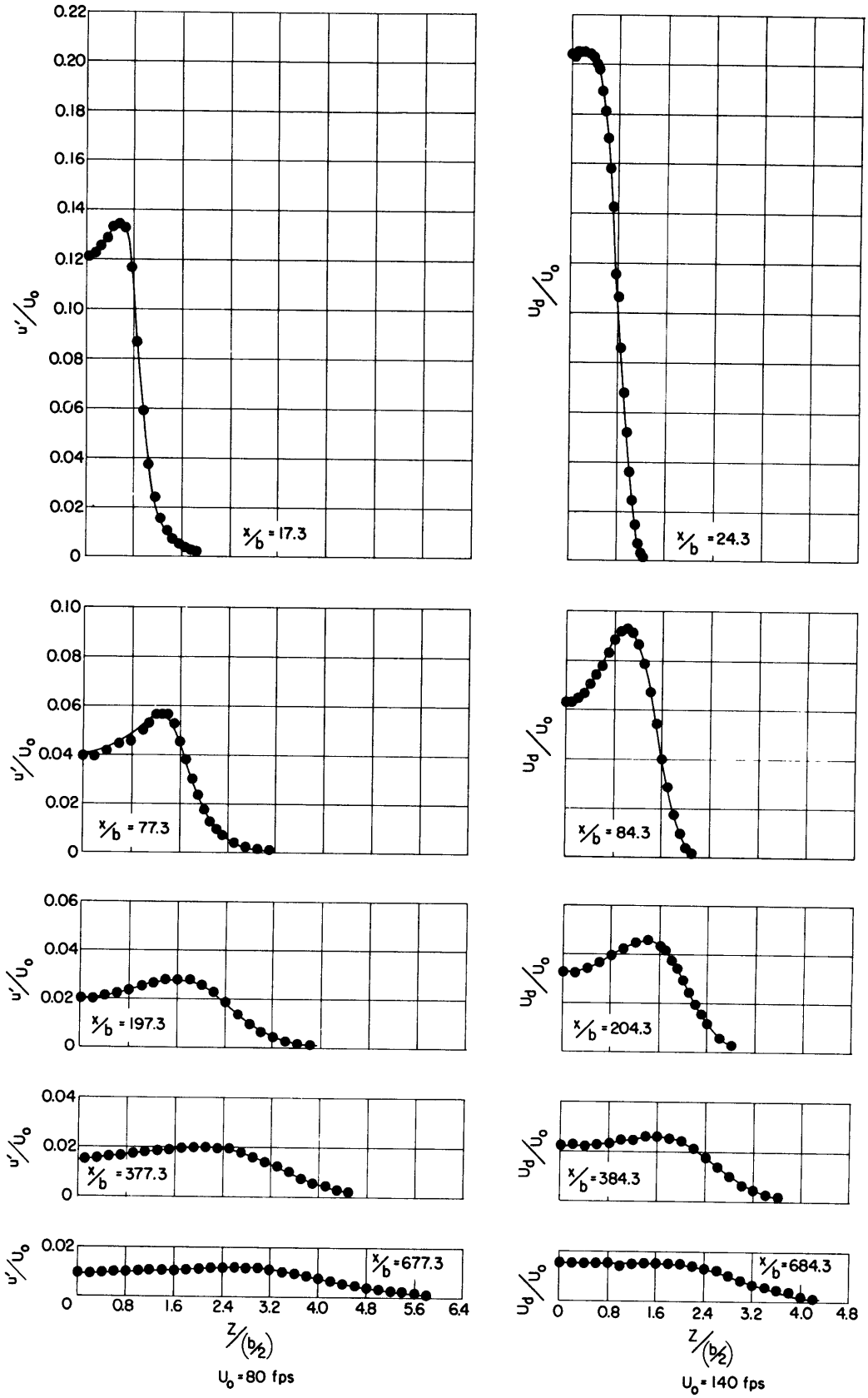

Figure 7 - Transverse Distributions of the Longitudinal Component of the Turbulent and Mean Velocity in the Wake behind Plate IV (l/b = 10, b = 0.2 Inch)

SIMILARITY ANALYSIS

A convenient way in which to analyze experimental data for the purpose of demonstrating similarity is (1) to investigate the value of the exponents α and β associated with the adjusting factors for the magnitude and length scales (see section on Theoretical Considerations, page 2) and (2) to examine the universality of the distribution function obtained when the basic data are reduced in accordance with these factors.

In the case of the wake velocities presently under consideration, the exponent α is readily determined from the variation with x of a characteristic velocity, e.g., the maximum velocity obtained in a given transverse distribution. In like manner, the exponent β is determined from the variation with x of a characteristic length, e.g., the distance $(z_{1/2})_f$ or $(z_{1/2})_m$ measured from the wake's axis of symmetry to the point in a given transverse distribution at which the turbulence intensity or the velocity defect, respectively, has one-half of its maximum value. (Although the actual size of the wake is a more natural choice for this characteristic length, the edge of the wake, in general, cannot be precisely determined and consequently is seldom used for this purpose.)

Figure 8 is a logarithmic representation of the variation with axial position of the maximum value of u'/U_0 measured in the wakes behind each of the test configurations. A similar representation of the maximum value of U_d/U_0 is given in Figure 9. For purposes of

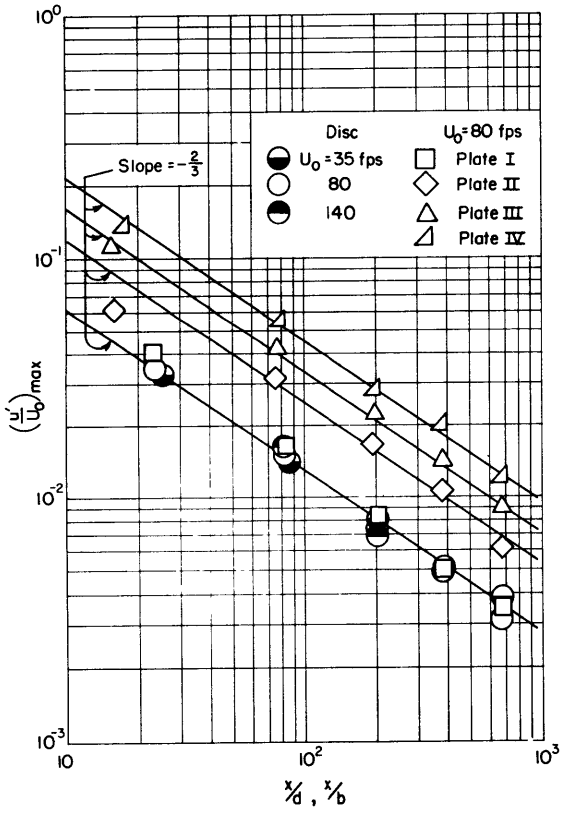

Figure 8 - Variation with Axial Position of $(u'/U_0)_{max}$

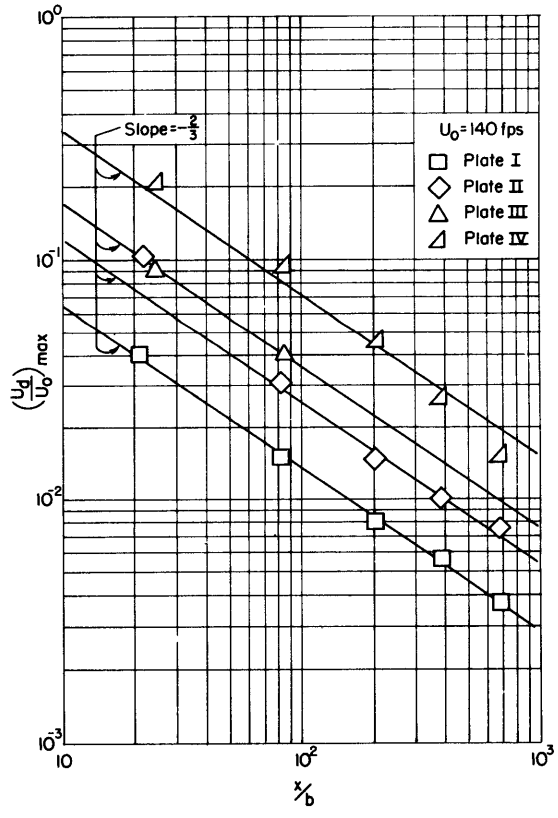

Figure 9 - Variation with Axial Position of $(U_d/U_0)_{max}$

comparison, straight lines with slopes equal to the negative two-thirds value, theoretically derived by similarity considerations of axially symmetric turbulent wakes, are drawn through each set of data. It is of interest to note that in the case of the turbulent velocity $(u'/U_0)_{max}$ very good agreement between theory and experiment is obtained not only for the disc and the square (Plate I) but also for the remaining configurations in spite of their marked departures from axial symmetry. Similarly, the comparison of the theoretical and experimental behavior of the mean velocity defect $(U_d/U_0)_{max}$ shows very good agreement, particularly in the case of Plate I. Some discrepancy, however, is noted in the case of Plate IV ($l/b = 10$) and is attributed to the axial asymmetry of the test configuration.

Figures 10 and 11 show the variation of the width of the fluctuating wake and the mean wake, respectively, as reflected by the lengths $(z_{1/2})_f$ and $(z_{1/2})_m$, which have been previously defined. Again, the straight lines on these logarithmic representations are indicative of the theoretically derived behavior of the axially symmetric wake width. The agreement between theory and experiment for both the turbulent and mean wakes is very good if, in the case of the higher aspect ratio configurations, experimental values obtained at the initial measuring stations are disregarded on the basis that the wake flow at these stations has not yet attained complete equilibrium.

In investigating the existence of universal velocity distribution functions the following technique was employed to reduce experimental scatter and thereby illustrate more effectively such universality for those cases in which it obtains. Faired curves, shown as solid lines in Figures 3 to 7, were drawn through each set of experimental velocity distributions and in the subsequent similarity analysis points taken from these curves were used, rather than the experimental points themselves. To be candid, the curves were faired with a considerable amount of hindsight where necessary; in general, however, the differences between faired curves and experimental data do no exceed the estimated precision of the data.

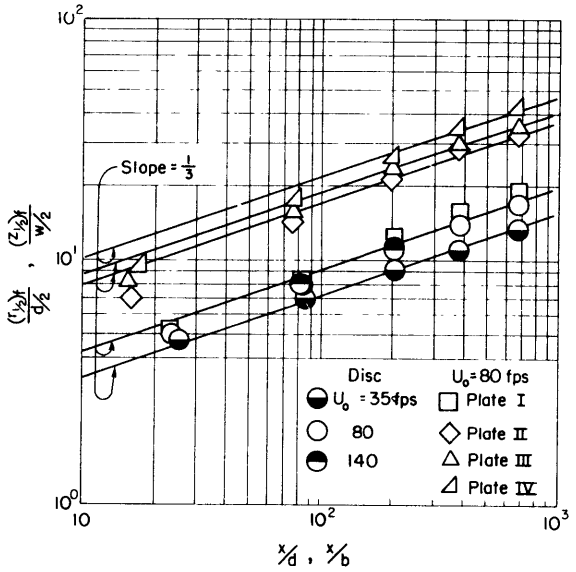

Figure 10 - Variation with Axial Position of the Width of the Fluctuating Wake

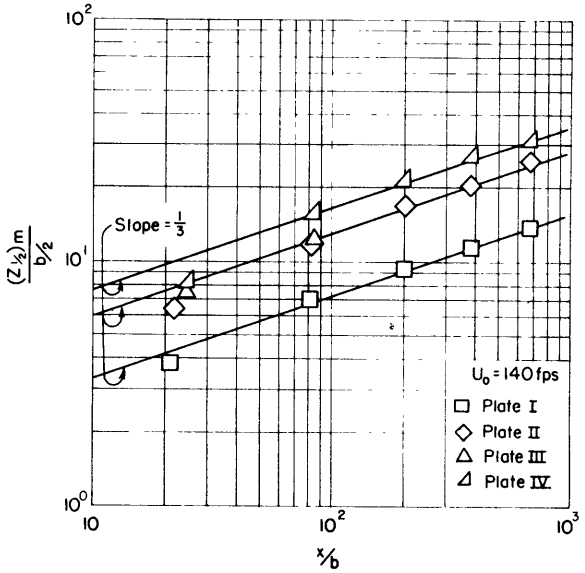

Figure 11 - Variation with Axial Position of the Width of the Mean Wake

Points taken from these faired curves are presented in the form u'/u'_{max} as a function of $r/(r_{1/2})_f$ or $z/(z_{1/2})_f$, as appropriate, in Figure 12 and in the form $U_d/U_{d\,max}$ as a function of $z/(z_{1/2})_m$ in Figure 13.

The mean velocity defect profiles of Plate I, which for present purposes can be considered as an axially symmetric configuration, are seen to be described by a universal distribution function; on the other hand, as obviously predictable from the basic data, such profiles for the three remaining plates are not similar. As previously indicated, this latter behavior reflects the three-dimensional nature of the mean wake behind axially asymmetric configurations. Although the trends are in the right direction, data were not obtained sufficiently far downstream to evaluate the intuitive expectation that such a wake would acquire axial symmetry in its downstream course and thereafter satisfy the similarity condition.

In view of these characteristics of the mean velocities, it is, at first, somewhat surprising to find that the fluctuating velocity profiles behind all of the test configurations do reduce to universal distribution functions as shown in Figure 12, and hence satisfy the similarity condition, at least to within the limits of precision of the experimental data. However, as a plausible partial explanation, it is suggested that the fluctuating wake reaches its equilibrium distribution very quickly, in spite of its interaction with the mean wake, which attains equilibrium much more slowly. In particular, this indicates that the energy transfer between the mean and fluctuating components of the flow is not critically dependent upon the precise shape of the mean velocity profile. This latter view is consistent with the previously ascertained result that $(U_d/U_0)_{max}$ varies in accordance with the theoretically predicted similarity law even in those cases in which the mean velocity defect profiles are not similar.

Figure 14 is a logarithmic representation of the variation with axial position of the microscale of turbulence λ, measured at transverse positions corresponding to points of maximum turbulence intensity in the wakes behind the various test configurations. This experimentally determined variation is adequately described by the ¼-power law, shown as a straight line in Figure 14, in contradiction of the ½-power law theoretically derived.

Because of its successful description of other wake flow characteristics, there is considerable reluctance to ascribe this variance between the measured and predicted behavior of λ to a failure of the similarity theory. The alternative interpretation is, of course, that the isotropic form of the dissipation function assumed in the theoretical analysis is in sufficient violation of the actual physical process to constitute a significantly erroneous representation. This latter explanation, however, is not substantiated in the results reported by J. Laufer;[11] these results, based on measurements made in a fully-developed turbulent pipe flow, indicate that the dissipation function is satisfactorily described by its isotropic form.

The simple, direct measurements of λ made in the present investigation unfortunately do not give any insight into the real nature of the dissipation function in wake flows; consequently, the difference between the theoretical prediction and the experimental determination of the behavior of λ must, for the present, remain unresolved.

(Text continued on page 22.)

Figure 12 - Representation of the Turbulence Intensity Distribution in Similarity Form

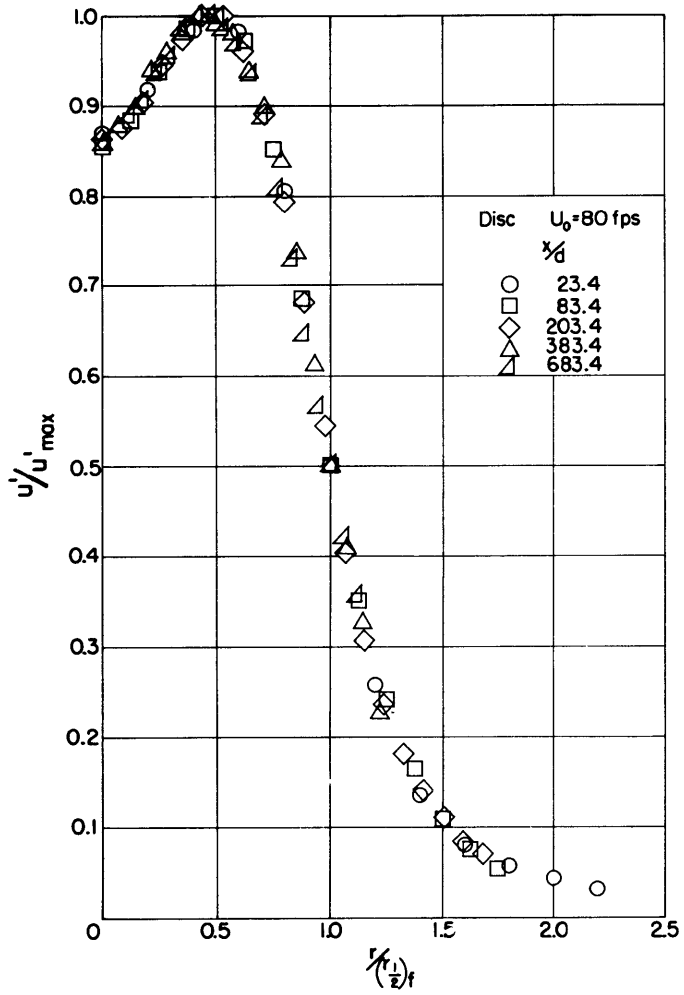

Figure 12a

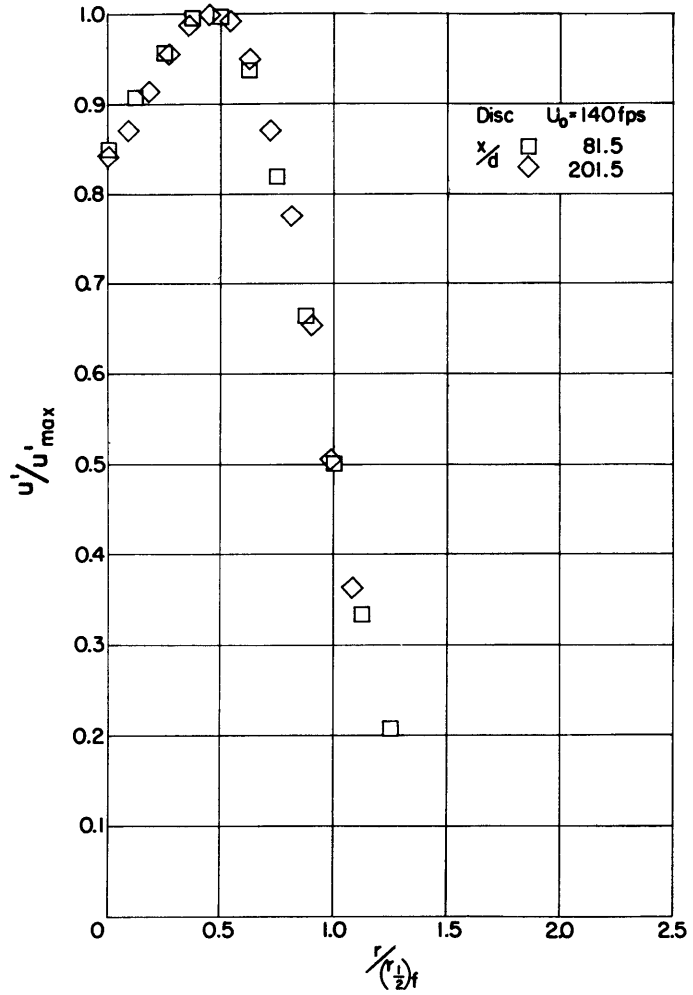

Figure 12b

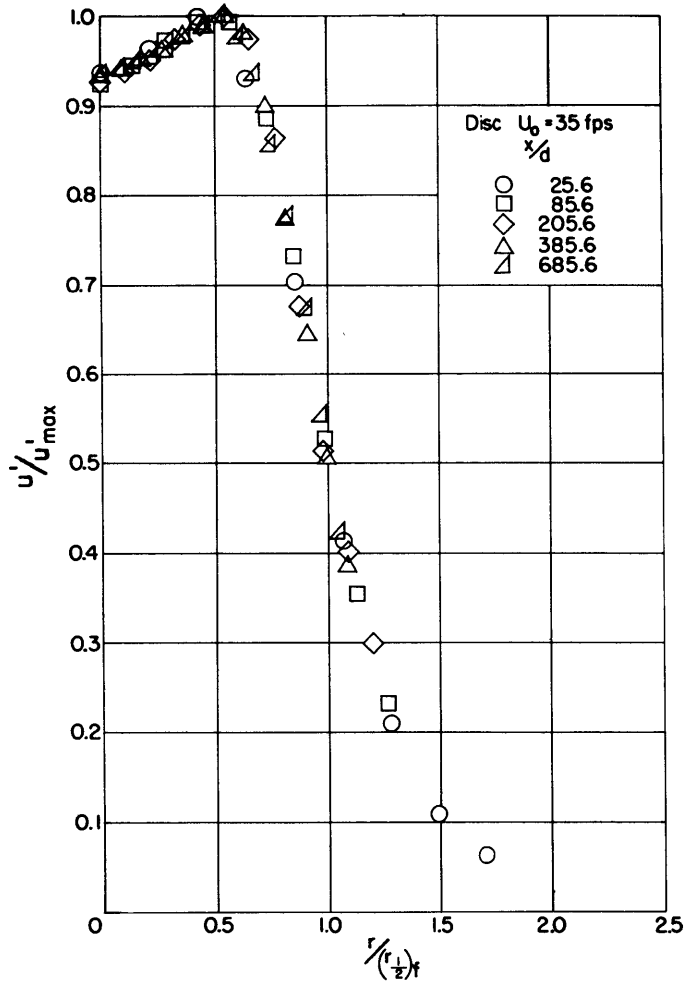

Figure 12c

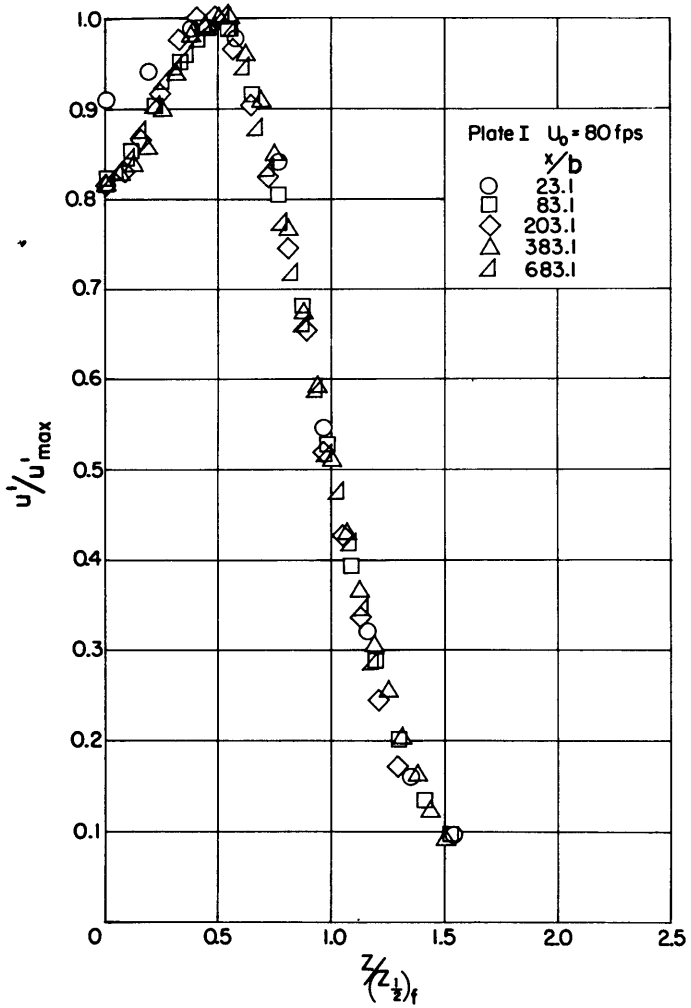

Figure 12d

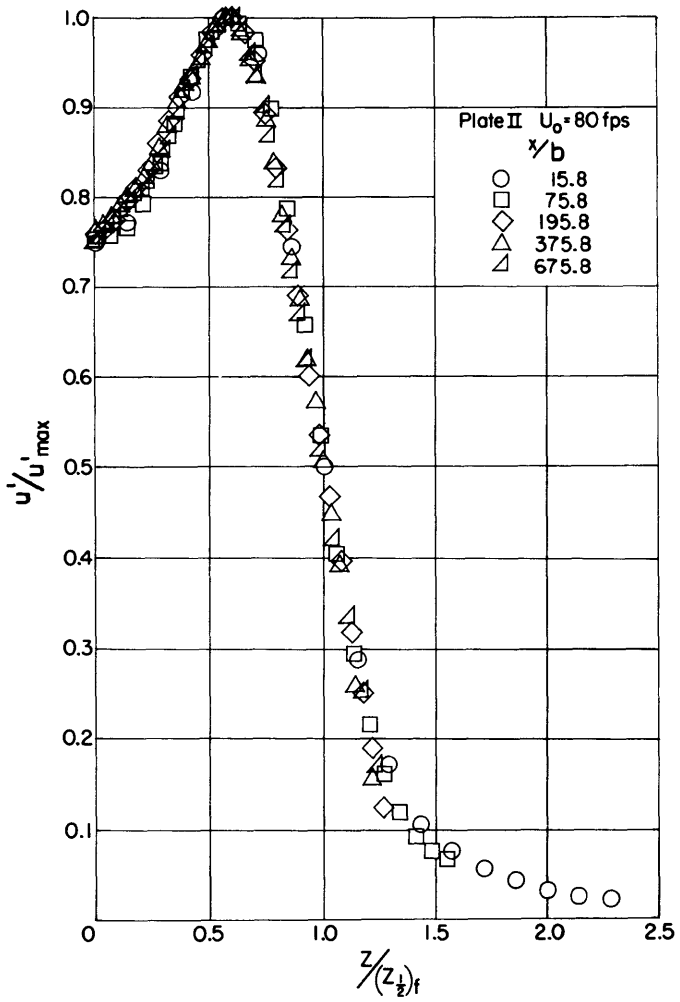

Figure 12e

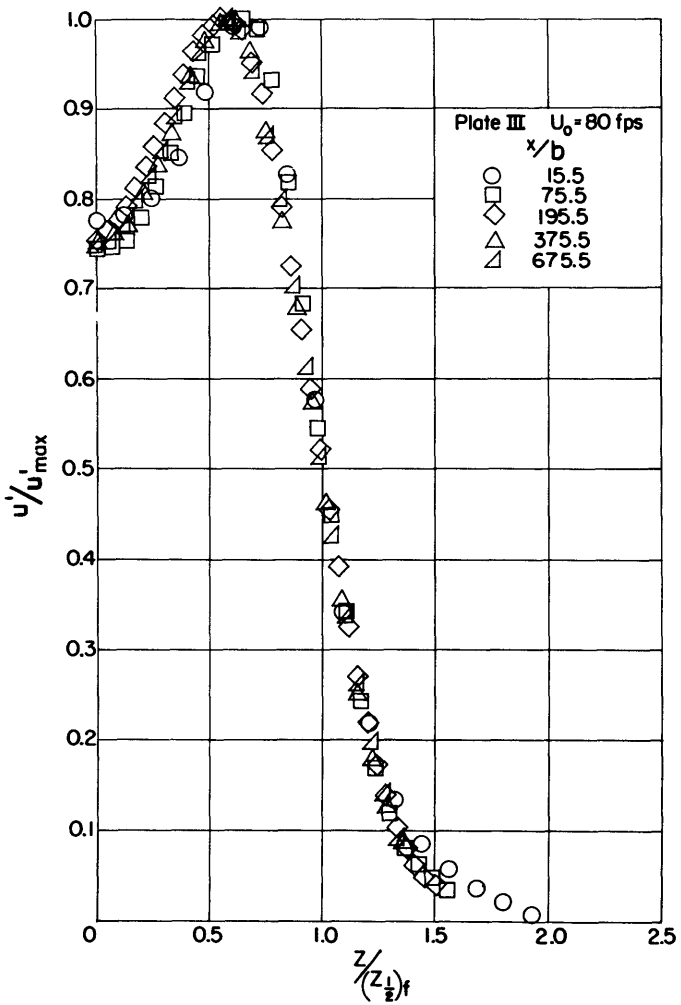

Figure 12f

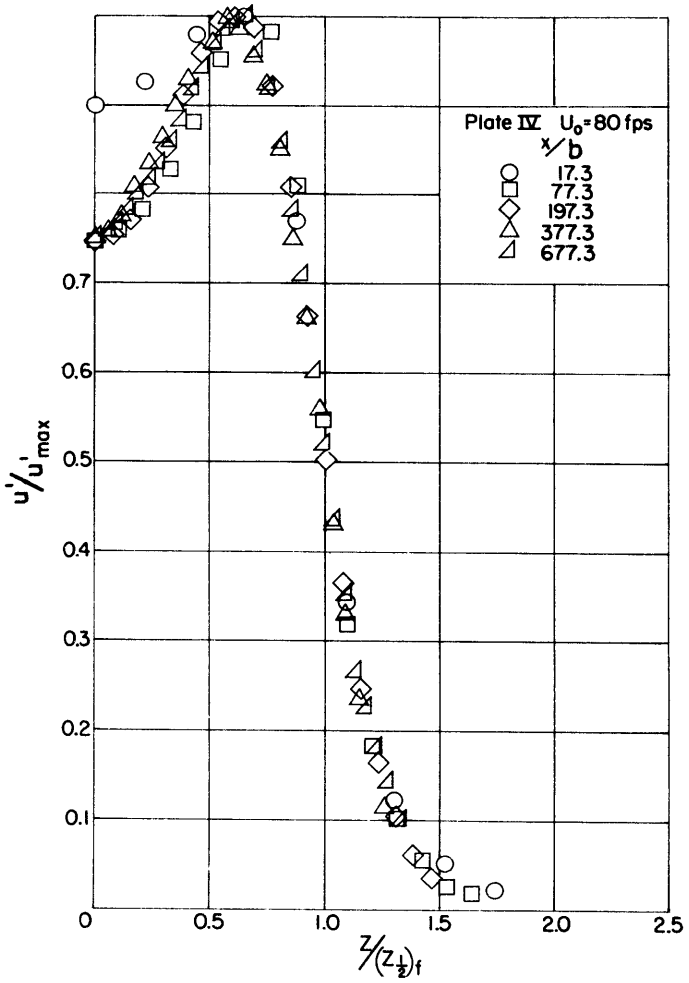
Plate IV U_o=80 fps
x/b
17.3
77.3
197.3
377.3
677.3
0.7
0.6
0.5
0.4
0.3
0.2
0.1
0
0.5
1.0
1.5
2.0
2.5
u'/u'_{max}
$z/(z_{\frac{1}{2}})_f$

Figure 12g

Figure 13 - Representations of the Mean Velocity Defect Distributions in Similarity Form

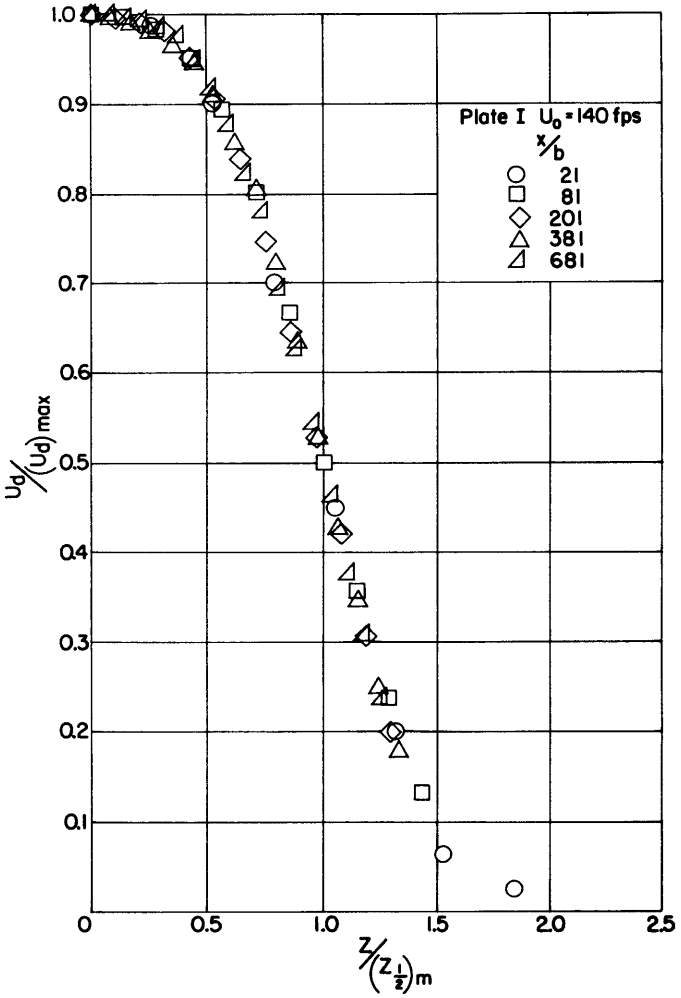

Figure 13a

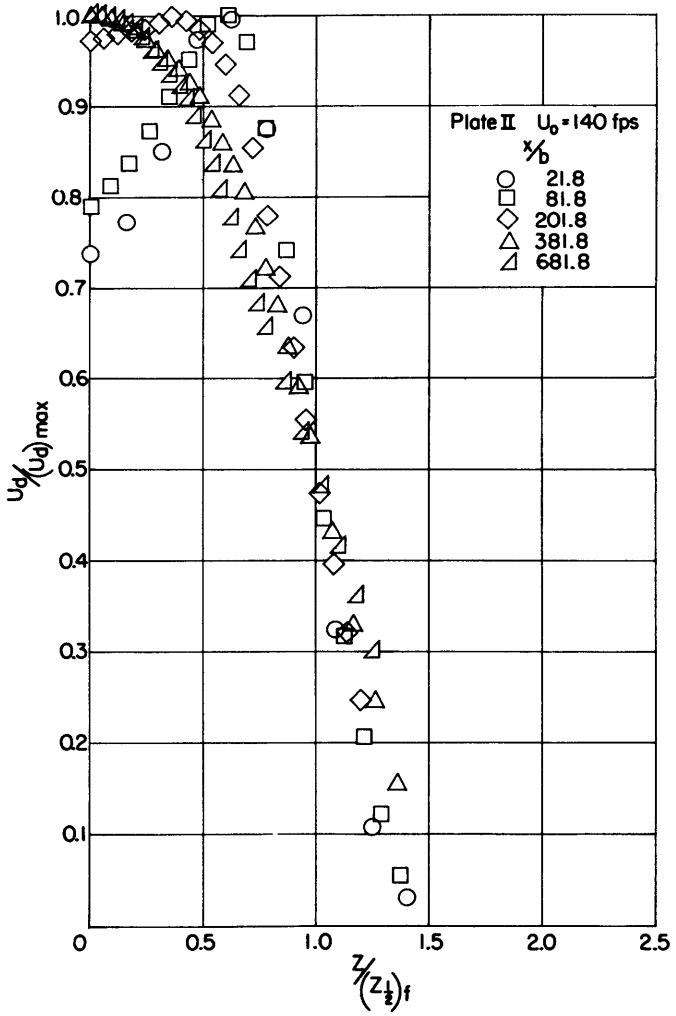

Figure 13b

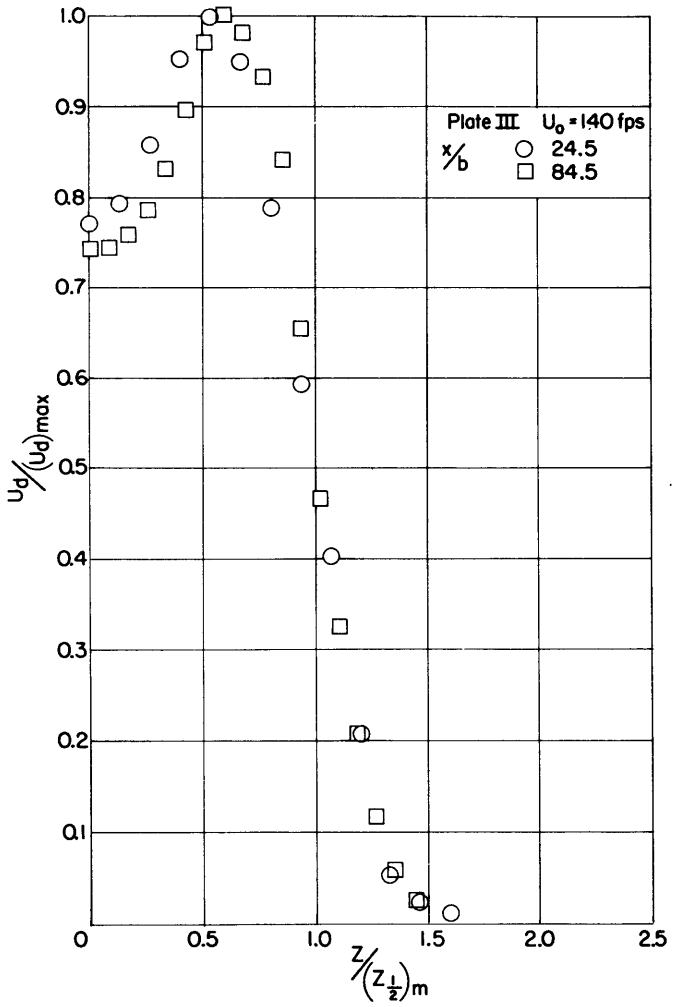

Figure 13c

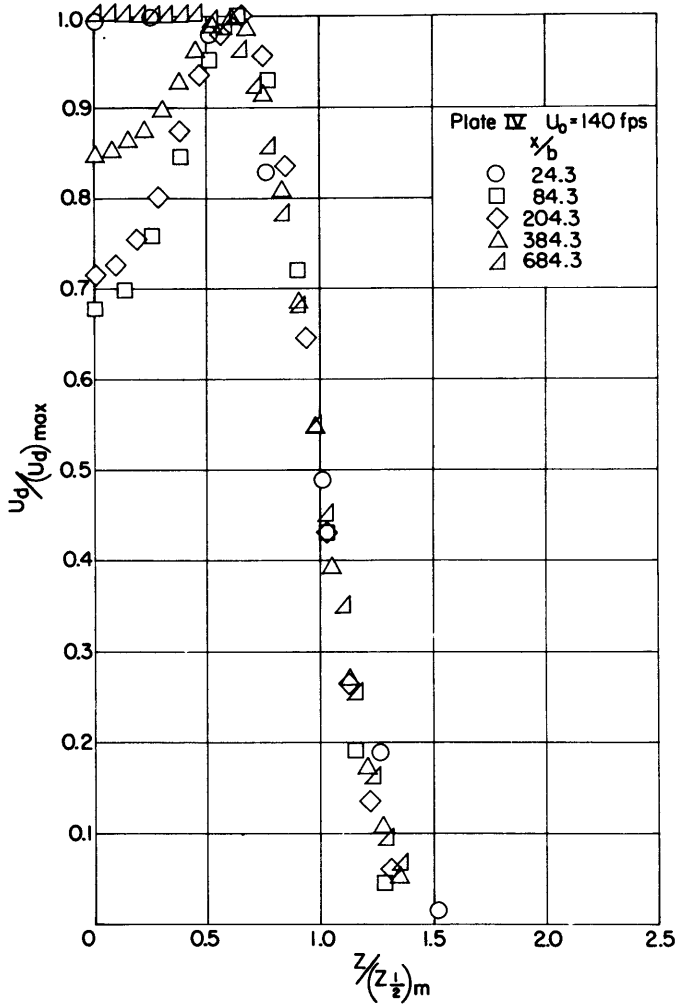

Figure 13d

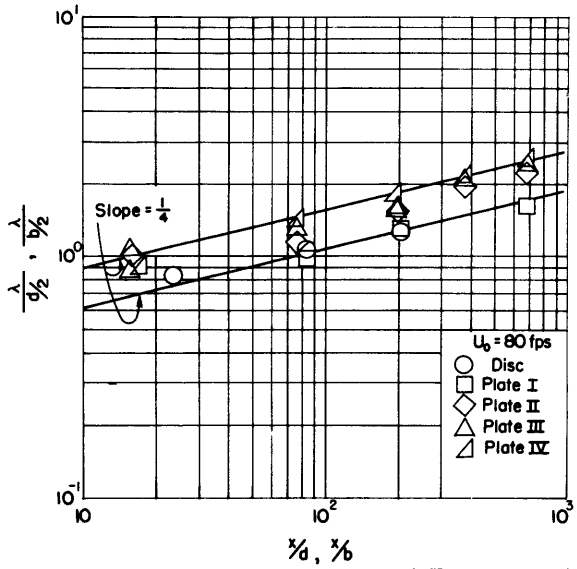

Figure 14 - Variation with Axial Position of λ at Transverse Location in Wake Corresponding to Maximum Turbulence Intensity

CONCLUSIONS

In the case of axially symmetric wakes, it is concluded that in agreement with the theoretical results derived from similarity considerations:

1. The maximum values of the mean velocity defect U_d and the turbulence intensity u' vary inversely as $x^{2/3}$.

2. The radius of the wake r_0 varies as $x^{1/3}$.

3. Transverse distributions of U_d and u' are universal functions of $\eta = r/x^{1/3}$.

It is further concluded that these results describe equally well the behavior of the corresponding characteristic quantities in the wakes behind the axially asymmetric plates tested, with the sole exception that the U_d-distributions of the higher aspect ratio plates do not describe universal functions.

Finally, the microscale of turbulence λ is found experimentally to vary as $x^{1/4}$ in contrast to the $x^{1/2}$ variation theoretically predicted from similarity considerations. This difference is at present unresolved.

APPENDIX A

THE REYNOLDS EQUATIONS OF MOTION AND THE ENERGY EQUATION OF TURBULENCE

DERIVATION

The motion of a viscous incompressible fluid is described by the Navier-Stokes equations which can be vectorially expressed as

$$\frac{\partial \mathbf{U}}{\partial t} + \mathbf{U} \cdot \nabla \mathbf{U} = -\frac{1}{\rho} \nabla P + \nu \nabla^2 \mathbf{U} \qquad [1A]$$

In addition, the fluid motion must also satisfy the continuity equation

$$\nabla \cdot \mathbf{U} = 0 \qquad [2A]$$

In these expressions, $\mathbf{U}$ is the velocity vector,

P is the pressure,

ρ is the density,

ν is the kinematic viscosity coefficient,

t is the time, and

∇ represents the conventional gradient operator which, of course, is a function of the coordinate system, denoted by $\mathbf{x}$ for brevity.

In accordance with a fundamental concept of turbulence, the so-called steady-state turbulent velocity field is separable into a mean motion and a fluctuating motion such that

$$\mathbf{U}(\mathbf{x}, t) = \mathbf{U}(\mathbf{x}) + \mathbf{u}(\mathbf{x}, t); \quad P(\mathbf{x}, t) = p(\mathbf{x}) + \tilde{p}(\mathbf{x}, t) \qquad [3A]$$

subject to the condition that temporal averages of the fluctuating quantities vanish, i.e.,

$$\mathbf{u} = \lim_{T \to \infty} \frac{1}{T} \int_{-T/2}^{T/2} \mathbf{u}\, dt = 0; \quad \tilde{\tilde{p}} = \lim_{T \to \infty} \frac{1}{T} \int_{-T/2}^{T/2} \tilde{p}\, dt = 0 \qquad [4A]$$

The Reynolds equations are obtained by introducing [3A] into [1A] and averaging with respect to time in the manner indicated by [4A]; the resulting equation can be expressed as

$$\mathbf{U} \cdot \nabla \mathbf{U} = -\frac{1}{\rho} \nabla p + \nu \nabla^2 \mathbf{U} - \overline{\mathbf{u} \cdot \nabla \mathbf{u}} \qquad [5A]$$

The manipulation of [2A] in an identical manner leads to the interesting and useful result that the continuity equation is separately satisfied by the mean motion and by the fluctuating motion, i.e.,

$$\nabla \cdot \mathbf{U} = 0; \quad \nabla \cdot \mathbf{u} = 0 \qquad [6A]$$

The so-called energy equation of turbulence is derived by subtracting the Reynolds equations [5A] from the Navier-Stokes equations [1A], after the latter has been expanded in accordance with the relations [3A]. Then, by forming the scaler product of $\mathbf{u}$ with each term of the resulting equation, an energy relation is obtained which, after manipulating with the aid

of [6A] and averaging with respect to time, takes the form

$$\mathbf{U}\cdot\nabla\,\overline{\frac{\mathbf{u}\cdot\mathbf{u}}{2}} = -\overline{\mathbf{u}\cdot(\mathbf{u}\cdot\nabla)\,\mathbf{U}} - \nabla\cdot\overline{\mathbf{u}\left(\frac{\mathbf{u}\cdot\mathbf{u}}{2}+\frac{\tilde{p}}{\rho}\right)} + \nu\,\overline{\mathbf{u}\cdot\nabla^2\mathbf{u}} \qquad [7A]$$

The last term in this equation represents the net effect of viscosity on the turbulent energy balance and is often expanded as

$$\nu\,\overline{\mathbf{u}\cdot\nabla^2\mathbf{u}} = \nu\left[\nabla^2\,\overline{\frac{\mathbf{u}\cdot\mathbf{u}}{2}} + \nabla\cdot\overline{(\mathbf{u}\cdot\nabla)\,\mathbf{u}}\right] - \nu\left[\nabla^2\,\overline{\frac{\mathbf{u}\cdot\mathbf{u}}{2}} + \nabla\cdot\overline{(\mathbf{u}\cdot\nabla)\,\mathbf{u}} - \overline{\mathbf{u}\cdot\nabla^2\mathbf{u}}\right] \qquad [8A]$$

In this form, the first bracketed expression is identifiable as the rate of transport of turbulent energy by viscous effects and the second is equal to the rate at which turbulent energy is dissipated to heat by the direct action of viscosity. (The interested reader is referred to Reference 12 for a more complete discussion of the viscous term in the energy equation.)

EXPANSION INTO CYLINDRICAL COORDINATES

In the cylindrical coordinate system described by x, r, θ, let U, V, W be mean velocity components and u, v, w, be fluctuating velocity components corresponding to the axial, radial, and tangential directions, respectively.

The continuity equation [6A] can then be expanded into

$$\frac{\partial U}{\partial x}+\frac{1}{r}\frac{\partial}{\partial r}rV+\frac{1}{r}\frac{\partial W}{\partial\theta}=0;\quad \frac{\partial u}{\partial x}+\frac{1}{r}\frac{\partial}{\partial r}rv+\frac{1}{r}\frac{\partial w}{\partial r}=0 \qquad [9A]$$

With the help of the last relation, the Reynolds equations [5A] can be expanded into

$$U\frac{\partial U}{\partial x}+V\frac{\partial U}{\partial r}+\frac{W}{r}\frac{\partial U}{\partial\theta} = -\frac{1}{\rho}\frac{\partial p}{\partial x}+\nu\left(\frac{\partial^2 U}{\partial x^2}+\frac{1}{r}\frac{\partial}{\partial r}r\frac{\partial U}{\partial r}+\frac{1}{r^2}\frac{\partial^2 U}{\partial\theta^2}\right)-\left(\frac{\partial\overline{u^2}}{\partial x}+\frac{1}{r}\frac{\partial}{\partial r}r\overline{uv}+\frac{1}{r}\frac{\partial\overline{uw}}{\partial\theta}\right)$$

$$U\frac{\partial V}{\partial x}+V\frac{\partial V}{\partial r}+\frac{W}{r}\frac{\partial V}{\partial\theta}-\frac{W^2}{r} = -\frac{1}{\rho}\frac{\partial p}{\partial r}+\nu\left(\frac{\partial^2 V}{\partial x^2}+\frac{1}{r}\frac{\partial}{\partial r}r\frac{\partial V}{\partial r}+\frac{1}{r^2}\frac{\partial^2 V}{\partial\theta^2}-\frac{V}{r^2}-\frac{2}{r^2}\frac{\partial W}{\partial\theta}\right)$$
$$-\left(\frac{\partial\overline{uv}}{\partial x}+\frac{1}{r}\frac{\partial}{\partial r}r\overline{v^2}+\frac{1}{r}\frac{\partial\overline{vw}}{\partial\theta}-\frac{\overline{w^2}}{r}\right) \qquad [10A]$$

$$U\frac{\partial W}{\partial x}+V\frac{\partial W}{\partial r}+\frac{W}{r}\frac{\partial W}{\partial\theta}+\frac{VW}{r} = -\frac{1}{\rho r}\frac{\partial p}{\partial\theta}+\nu\left(\frac{\partial^2 W}{\partial x}+\frac{1}{r}\frac{\partial}{\partial r}r\frac{\partial W}{\partial r}+\frac{1}{r^2}\frac{\partial^2 W}{\partial\theta^2}-\frac{W}{r^2}+\frac{2}{r^2}\frac{\partial W}{\partial\theta}\right)$$
$$-\left(\frac{\partial\overline{uw}}{\partial x}+\frac{1}{r}\frac{\partial}{\partial r}r\overline{vw}+\frac{1}{r}\frac{\partial\overline{w^2}}{\partial\theta}+\frac{\overline{vw}}{r}\right)$$

Similarly, the energy equation of turbulence [7A] with the viscous term replaced by the identity [8A] expands into

$$\left(U\frac{\partial}{\partial x}+V\frac{\partial}{\partial r}+\frac{W}{r}\frac{\partial}{\partial\theta}\right)\left(\frac{\overline{u^2}+\overline{v^2}+\overline{w^2}}{2}\right)=-\left(\overline{u^2}\frac{\partial U}{\partial x}+\overline{uv}\frac{\partial U}{\partial r}+\frac{\overline{uw}}{r}\frac{\partial U}{\partial\theta}\right)$$

$$-\left(\overline{uv}\frac{\partial V}{\partial x}+\overline{v^2}\frac{\partial V}{\partial r}+\frac{\overline{vw}}{r}\frac{\partial V}{\partial\theta}-\frac{\overline{vw}}{r}W\right)-\left(\overline{uw}\frac{\partial W}{\partial x}+\overline{vw}\frac{\partial W}{\partial r}+\frac{\overline{w^2}}{r}\frac{\partial W}{\partial\theta}+\frac{\overline{w^2}}{r}V\right)$$

$$+\frac{\partial}{\partial x}\left\{\nu\left[\frac{\partial}{\partial x}\left(\frac{\overline{u^2}+\overline{v^2}+\overline{w^2}}{2}\right)+\frac{\partial\overline{u^2}}{\partial x}+\frac{1}{r}\frac{\partial}{\partial r}r\overline{uv}+\frac{1}{r}\frac{\partial\overline{uw}}{\partial\theta}\right]-\overline{u\left(\frac{u^2+v^2+w^2}{2}+\frac{\widetilde{p}}{\rho}\right)}\right\} \qquad [11A]$$

$$+\frac{1}{r}\frac{\partial}{\partial r}r\left\{\nu\left[\frac{\partial}{\partial r}\left(\frac{\overline{u^2}+\overline{v^2}+\overline{w^2}}{2}\right)+\frac{\partial\overline{uv}}{\partial x}+\frac{1}{r}\frac{\partial}{\partial r}r\overline{v^2}+\frac{1}{r}\frac{\partial\overline{vw}}{\partial\theta}-\frac{\overline{w^2}}{r}\right]-\overline{v\left(\frac{u^2+v^2+w^2}{2}+\frac{\widetilde{p}}{\rho}\right)}\right\}$$

$$+\frac{1}{r}\frac{\partial}{\partial\theta}\left\{\nu\left[\frac{1}{r}\frac{\partial}{\partial\theta}\left(\frac{\overline{u^2}+\overline{v^2}+\overline{w^2}}{2}\right)+\frac{\partial\overline{uw}}{\partial x}+\frac{1}{r}\frac{\partial}{\partial r}r\overline{vw}+\frac{1}{r}\frac{\partial\overline{w^2}}{\partial\theta}-\frac{\overline{vw}}{r}\right.\right.-\left.\left.\overline{w\left(\frac{u^2+v^2+w^2}{2}+\frac{\widetilde{p}}{\rho}\right)}\right\}$$

$$-\nu\left[2\overline{\left(\frac{\partial u}{\partial x}\right)^2}+2\overline{\left(\frac{\partial v}{\partial r}\right)^2}+2\overline{\left(\frac{1}{r}\frac{\partial w}{\partial\theta}+\frac{v}{r}\right)^2}+\overline{\left(\frac{\partial u}{\partial r}+\frac{\partial v}{\partial x}\right)^2}+\overline{\left(\frac{\partial w}{\partial x}+\frac{1}{r}\frac{\partial u}{\partial\theta}\right)^2}+\overline{\left(\frac{\partial w}{\partial r}+\frac{1}{r}\frac{\partial v}{\partial\theta}-\frac{w}{r}\right)^2}\right]$$

SIMPLIFICATION IN THE CASE OF AXIAL SYMMETRY

In an axially symmetric flow, the mean tangential velocity component W together with all derivatives with respect to θ of mean and averaged quantities vanish identically.

Consequently, the continuity equation [9A] simplifies to

$$\frac{\partial U}{\partial x}+\frac{1}{r}\frac{\partial}{\partial r}rV=0;\quad \frac{\partial u}{\partial x}+\frac{1}{r}\frac{\partial}{\partial r}rv+\frac{1}{r}\frac{\partial w}{\partial\theta}=0 \qquad [12A]$$

the Reynolds equations [10A] simplify to

$$U\frac{\partial U}{\partial x}+V\frac{\partial U}{\partial r}=-\frac{1}{\rho}\frac{\partial p}{\partial x}+\nu\left(\frac{\partial^2U}{\partial x^2}+\frac{1}{r}\frac{\partial}{\partial r}r\frac{\partial U}{\partial r}\right)-\left(\frac{\partial\overline{u^2}}{\partial x}+\frac{1}{r}\frac{\partial}{\partial r}r\overline{uv}\right),$$

$$U\frac{\partial V}{\partial x}+V\frac{\partial V}{\partial r}=-\frac{1}{\rho}\frac{\partial p}{\partial r}+\nu\left(\frac{\partial^2V}{\partial x^2}+\frac{1}{r}\frac{\partial}{\partial r}r\frac{\partial V}{\partial r}-\frac{V}{r^2}\right)-\left(\frac{\partial\overline{uv}}{\partial x}+\frac{1}{r}\frac{\partial}{\partial r}r\overline{v^2}-\frac{\overline{w^2}}{r}\right), \qquad [13A]$$

$$0=\frac{\partial\overline{uw}}{\partial x}+\frac{1}{r}\frac{\partial}{\partial r}r\overline{vw}+\frac{\overline{vw}}{r}$$

and the energy equation [11A] simplifies to

$$\left(U\frac{\partial}{\partial x}+V\frac{\partial}{\partial r}\right)\left(\frac{\overline{u^2}+\overline{v^2}+\overline{w^2}}{2}\right)=-\left(\overline{u^2}\frac{\partial U}{\partial x}+\overline{uv}\frac{\partial U}{\partial r}\right)-\left(\overline{uv}\frac{\partial V}{\partial x}+\overline{v^2}\frac{\partial V}{\partial r}+\overline{w^2}\frac{V}{r}\right)$$

$$+\frac{\partial}{\partial x}\left\{\nu\left[\frac{\partial}{\partial x}\left(\frac{\overline{u^2}+\overline{v^2}+\overline{w^2}}{2}\right)+\frac{\partial\overline{u^2}}{\partial x}+\frac{1}{r}\frac{\partial}{\partial r}\,r\overline{uv}\right]-\overline{u\left(\frac{u^2+v^2+w^2}{2}+\frac{\widetilde{p}}{\rho}\right)}\right\} \qquad [14A]$$

$$+\frac{1}{r}\frac{\partial}{\partial r}r\left\{\nu\left[\frac{\partial}{\partial r}\left(\frac{\overline{u^2}+\overline{v^2}+\overline{w^2}}{2}\right)+\frac{\partial\overline{uv}}{\partial x}+\frac{1}{r}\frac{\partial}{\partial r}r\overline{v^2}-\frac{\overline{w^2}}{r}\right]-\overline{v\left(\frac{u^2+v^2+w^2}{2}+\frac{\widetilde{p}}{\rho}\right)}\right\}$$

$$-\nu\left[2\overline{\left(\frac{\partial u}{\partial x}\right)^2}+2\overline{\left(\frac{\partial v}{\partial r}\right)^2}+2\overline{\left(\frac{1}{r}\frac{\partial w}{\partial\theta}+\frac{v}{r}\right)^2}+\overline{\left(\frac{\partial u}{\partial r}+\frac{\partial v}{\partial x}\right)^2}+\overline{\left(\frac{\partial w}{\partial x}+\frac{1}{r}\frac{\partial u}{\partial\theta}\right)^2}+\overline{\left(\frac{\partial w}{\partial r}+\frac{1}{r}\frac{\partial v}{\partial\theta}-\frac{w}{r}\right)^2}\right]$$

APPENDIX B

DERIVATION OF APPROXIMATE EQUATIONS OF FLUID MOTION

In the case of an axially symmetric turbulent wake, the exact equations governing the fluid motion may be replaced with approximate equations which are deduced from the former by an order-of-magnitude analysis similar to that applied in boundary layer flows.

As a preliminary step toward this end, it is convenient to introduce into the exact equation the so-called mean velocity defect $U_d = U_0 - U$ and to nondimensionalize the resulting set of equations by means of the free stream velocity U_0 and an arbitrary, but fixed axial length x_0. Then, Equations [12A], [13A], and [14A] can be rewritten as

$$\frac{\partial U_{d_1}}{\partial x_1} - \frac{1}{r_1}\frac{\partial}{\partial r_1} r_1 V_1 = 0; \quad \frac{\partial u_1}{\partial x_1} + \frac{1}{r_1}\frac{\partial}{\partial r_1} r_1 v_1 + \frac{1}{r_1}\frac{\partial w_1}{\partial \theta} = 0 \qquad [1B]$$

$$(1 - U_{d_1})\frac{\partial U_{d_1}}{\partial x_1} + V_1 \frac{\partial U_{d_1}}{\partial r_1} = \frac{\partial}{\partial x_1}\frac{p}{\rho U_0^2} + \frac{\nu}{U_0 x_0}\left(\frac{\partial^2 U_{d_1}}{\partial x_1} + \frac{1}{r_1}\frac{\partial}{\partial r_1} r_1 \frac{\partial U_{d_1}}{\partial r_1}\right) + \left(\frac{\partial \overline{u_1^2}}{\partial x_1} + \frac{1}{r_1}\frac{\partial}{\partial r_1} r_1 \overline{u_1 v_1}\right)$$

$$(1 - U_{d_1})\frac{\partial V_1}{\partial x_1} + V_1 \frac{\partial V_1}{\partial r_1} = -\frac{\partial}{\partial r_1}\frac{p}{\rho U_0^2} + \frac{\nu}{U_0 x_0}\left(\frac{\partial^2 V_1}{\partial x_1} + \frac{1}{r_1}\frac{\partial}{\partial r_1} r_1 \frac{\partial V_1}{\partial r_1}\right) - \left(\frac{\partial \overline{u_1 v_1}}{\partial x_1} + \frac{1}{r_1}\frac{\partial}{\partial r_1} r_1 \overline{v_1^2} - \frac{\overline{w_1^2}}{r_1}\right) \qquad [2B]$$

$$0 = \frac{\partial \overline{u_1 w_1}}{\partial x_1} + \frac{1}{r_1}\frac{\partial}{\partial r_1} r_1 \overline{v_1 w_1} + \frac{\overline{v_1 w_1}}{r_1}$$

$$\left[(1 - U_{d_1})\frac{\partial}{\partial x_1} + V_1 \frac{\partial}{\partial r_1}\right]\left(\frac{\overline{u_1^2} + \overline{v_1^2} + \overline{w_1^2}}{2}\right) = \overline{u_1^2}\frac{\partial U_{d_1}}{\partial x_1} + \overline{u_1 v_1}\frac{\partial U_{d_1}}{\partial r_1} - \overline{u_1 v_1}\frac{\partial V_1}{\partial x_1} - \overline{v_1^2}\frac{\partial V_1}{\partial r_1} \qquad [3B]$$

$$- \overline{w_1^2}\frac{V_1}{r_1} + \frac{\partial}{\partial x_1}\left\{\frac{\nu}{U_0 x_0}\left[\frac{\partial}{\partial x_1}\left(\frac{\overline{u_1^2} + \overline{v_1^2} + \overline{w_1^2}}{2}\right) + \frac{\partial \overline{u_1^2}}{\partial x_1} + \frac{1}{r_1}\frac{\partial}{\partial r_1} r_1 \overline{u_1 v_1}\right] - \overline{u_1\left(\frac{u_1^2 + v_1^2 + w_1^2}{2} + \frac{\widetilde{p}}{\rho U_0^2}\right)}\right\}$$

$$+ \frac{1}{r_1}\frac{\partial}{\partial r_1} r_1\left\{\frac{\nu}{U_0 x_0}\left[\frac{\partial}{\partial r_1}\left(\frac{\overline{u_1^2} + \overline{v_1^2} + \overline{w_1^2}}{2}\right) + \frac{\partial \overline{u_1 v_1}}{\partial x_1} + \frac{1}{r_1}\frac{\partial}{\partial r_1} r_1 \overline{v_1^2} - \frac{\overline{w_1^2}}{r_1}\right] - \overline{v_1\left(\frac{u_1^2 + v_1^2 + w_1^2}{2} + \frac{\widetilde{p}}{\rho U_0^2}\right)}\right\}$$

$$+ \frac{\nu}{U_0 x_0}\left[2\overline{\left(\frac{\partial u_1}{\partial x_1}\right)^2} + 2\overline{\left(\frac{\partial v_1}{\partial r_1}\right)^2} + 2\overline{\left(\frac{\partial w_1}{r_1 \partial \theta} + \frac{v_1}{r_1}\right)^2} + \overline{\left(\frac{\partial u_1}{\partial r_1} + \frac{\partial v_1}{\partial x_1}\right)^2} + \overline{\left(\frac{\partial w_1}{\partial x_1} + \frac{\partial u_1}{r_1 \partial \theta}\right)^2} + \overline{\left(\frac{\partial w_1}{\partial r_1} + \frac{\partial v_1}{r_1 \partial \theta} - \frac{w_1}{r_1}\right)^2}\right]$$

where the subscript 1 indicates a quantity nondimensionalized with U_0 or x_0, as applicable.

The numerical value of U_{d_1} is chosen as a reference and assigned an order of magnitude ϵ, where ϵ is small in comparison with unity, i.e., $\epsilon \ll 1$. Then x_0 is so selected that the values of r_1 encountered in the wake are of the same order of magnitude as U_{d_1}, i.e., $r_1 = O(\epsilon)$.

Finally, the axial interval of the wake to be considered is restricted to that interval in which $x_1 = O(1)$.

It is then apparent from the continuity equation [1B] that $V_1 = O(\epsilon)$.

Using this result and replacing terms where possible with their order of magnitude values, the first two equations of the set [2B] can be written as

$$(1-\epsilon)\epsilon + \epsilon^2 \cdot 1 = 1 \cdot \frac{p}{\rho U_0^2} + \frac{\nu}{U_0 x_0}(\epsilon + \epsilon^{-1}) + (1 \cdot \overline{u_1^2} + \overline{u_1 v_1} \cdot \epsilon^{-1})$$

$$(1-\epsilon)\epsilon^2 + \epsilon^2 \cdot \epsilon = -\epsilon^{-1}\frac{p}{\rho U_0^2} + \frac{\nu}{U_0 x_0}(\epsilon^2 + 1) + (1 \cdot \overline{u_1 v_1} + \epsilon^{-1} \cdot \overline{v_1^2} - \epsilon^{-1}\,\overline{w_1^2}) \qquad [4B]$$

Since a turbulent wake is under consideration, it is implied that the forces due to the turbulence stresses are of the same order of magnitude as the inertial forces, while the viscous forces must be at least another order of magnitude smaller. Consequently, assuming that all elements of the Reynolds stress tensor are of the same order of magnitude, the first of Equations [4B] indicates that these elements must be $O(\epsilon^2)$; at the same time, this equation indicates that $(\nu/U_0 x_0) = O(\epsilon^3)$.

Using these results in the second equation of [4B], a conservative estimate of the pressure term can be made by assigning to it an order of magnitude equal to that of the largest of the other component terms of the equation. In this way, it is easily shown that $p/(\rho U_0^2) = O(\epsilon^2)$.

For an axially symmetric turbulent wake, a first approximation to the exact Reynolds equations is obtained by discarding all terms of order ϵ^2 and higher, and can be written as

$$\frac{\partial U_{d_1}}{\partial x_1} = \frac{1}{r_1}\frac{\partial}{\partial r_1} r_1 \overline{u_1 v_1} \qquad [5B]$$

With the additional assumptions that $\widetilde{p}/(\rho U_0^2)$ is of the order ϵ^2 or smaller and that the viscous dissipation term is of the same order as the largest of the other component terms in the equation, a first approximation to the energy equation [3B] can be derived in the same way and written as

$$\frac{\partial}{\partial x_1}\left(\frac{\overline{u_1^2} + \overline{v_1^2} + \overline{w_1^2}}{2}\right) = \overline{u_1 v_1}\,\frac{\partial U_{d_1}}{\partial r_1} + \frac{\nu}{U_0 x_0}\Phi_1 \qquad [6B]$$

where

$$\Phi_1 = 2\overline{\left(\frac{\partial u_1}{\partial x_1}\right)^2} + 2\overline{\left(\frac{\partial v_1}{\partial r_1}\right)^2} + 2\overline{\left(\frac{\partial w_1}{r_1 \partial \theta} + \frac{v_1}{r_1}\right)^2} + \overline{\left(\frac{\partial u_1}{\partial r_1} + \frac{\partial v_1}{\partial x_1}\right)^2} + \overline{\left(\frac{\partial w_1}{\partial x_1} + \frac{\partial u_1}{r_1 \partial \theta}\right)^2} + \overline{\left(\frac{\partial w_1}{\partial r_1} + \frac{\partial v_1}{r_1 \partial \theta} - \frac{w_1}{r_1}\right)^2}$$

If it is assumed that the nondimensionalized dissipation function Φ_1 can be satisfactorily approximated by its isotropic form, i.e., $\Phi_1 = (15\overline{u_1^2})/\lambda_1^2$, it can be shown that $\lambda_1^2/15$ must be of order ϵ^3 in order that the dissipation term in [6B] have the same order of magnitude as the other terms.

Thus, in recapitulation, a first order approximation to the Reynolds equations in the case under consideration is

$$U_0 \frac{\partial U_d}{\partial x} = \frac{1}{r} \frac{\partial}{\partial r} r\overline{uv} \qquad [7B]$$

a similar approximation to the energy equation is

$$U_0 \frac{\partial}{\partial x}\left(\frac{\overline{u^2} + \overline{v^2} + \overline{w^2}}{2}\right) = \overline{uv} \frac{\partial U_d}{\partial r} + \nu\Phi$$

or, if Φ be given its isotropic form,

$$U_0 \frac{\partial}{\partial x}\left(\frac{\overline{u^2} + \overline{v^2} + \overline{w^2}}{2}\right) = \overline{uv} \frac{\partial U_d}{\partial r} + \frac{15\nu\overline{u^2}}{\lambda^2} \qquad [8B]$$

It is of interest to examine the experimental data obtained in the wakes behind the disc and the square in the light of the order of magnitude analysis presented above. The pertinent data can be conveniently summarized as follows:

5	inches	$< x <$	140	inches
1	inch	$< r <$	2	inches
0.004		$< u_1' <$	0.04	
0.004		$< U_{d_1} <$	0.04	
0.06	inch	$< \lambda <$	0.16	inch

In order to satisfy the condition that $x_1 = O(1)$ over that interval of the wake in which the data were taken, x_0 is set at 5 feet. It then follows that $0.016 < r_1 < 0.033$, $0.6 \times 10^{-7} < \lambda_1^2/15 < 4.5 \times 10^{-7}$, and $\nu/U_0 x_0 \approx 4 \times 10^{-7}$ if $U_0 = 80$ fps and $\nu = 1.5 \times 10^{-4}$ ft^2/sec. Hence, it is seen that u_1, r_1, and U_{d_1} are of the same order of magnitude which, if denoted by ϵ, satisfies the condition that $\epsilon \ll 1$, as required in the analysis. It is further seen that both $\nu/U_0 x_0$ and $\lambda_1^2/15$ are of order ϵ^3, which is consistent with and in support of the assumptions involved in the derivation of Equations [7B] and [8B].

REFERENCES

1. Reynolds, O., "On the Dynamical Theory of Incompressible Viscous Fluids and the Determination of the Criterion," Philosophical Transactions of the Royal Society of London, Serial A, Vol. 186 (1895), pp. 123-164.

2. Batchelor, G.K. and Townsend, A.A., "Decay of Isotropic Turbulence in the Initial Period," Proceedings of the Royal Society, London, Serial A, Vol. 193, No. 1035 (Jul 21, 1948) pp 539-558.

3. Batchelor, G.K. and Townsend, A.A., "Decay of Turbulence in the Final Period," Proceedings of the Royal Society, London, Serial A, Vol. 194, No. 1039 (Nov 9, 1948), pp. 527-543.

4. Corrsin, Stanley, "Investigation of Flow in an Axially Symmetrical Heated Jet of Air," NACA ACR 3L23 (1943).

5. Corrsin, Stanley and Uberoi, Mahinder S., "Further Experiments on the Flow and Heat Transfer in a Heated Turbulent Air Jet," NACA TN 1865 (1949).

6. Townsend, A.A., "Measurements in the Turbulent Wake of a Cylinder," Proceedings of the Royal Society, London, Serial A, Vol. 190, No. 1023 (Sep 9, 1947), pp. 551-561.

7. Townsend, A.A., "The Fully Developed Turbulent Wake of a Circular Cylinder," Australian Journal of Scientific Research, Serial A, Vol. 2 (1949), pp. 451-468.

8. Prandtl, L., "Ueber die ausgebildete Turbulenz," Proceedings of the Second International Congress of Applied Mechanics, Zurich (1926), pp. 62-74.

9. Taylor, G.I. with an Appendix by Fage, A. and Falkner, V.M., "Transport of Vorticity and Heat through Fluids in Turbulent Motion," Proceedings of the Royal Society, London, Serial A, Vol. 135 (1932), pp. 685-705.

10. von Kármán, Th., "Mechanische Ahnlichkeit und Turbulenz," Proceedings of the Third International Congress of Applied Mechanics, Stockholm, Vol. 1 (1930), pp. 85-93.

11. Laufer, John, "The Structure of Turbulence in Fully Developed Pipe Flow," NACA TN 2954 (1953).

12. Corrsin, Stanley, "Interpretation of Viscous Terms in the Turbulent Energy Equation," Journal of Aeronautical Science, Vol. 20, No. 12 (Dec 1953), pp. 853-854.

INITIAL DISTRIBUTION

Copies

6 Chief, BuShips, Library (Code 312)
  5 Technical Library
  1 Tech Asst to Chief (Code 106)

2 Chief, BuOrd, Re6a

2 Chief, BuAer

2 Chief of Naval Research (Code 438)

2 DIR, USNRL

2 CDR, USNOL

2 CDR, USNOTS, Inyokern, Calif.
  1 Pasadena Annex

2 ASTIA, Dayton, Ohio

5 DIR, NACA

1 Bassin d'Essais des Carènes, Paris, France

1 Office National d'Études et de Recherches Aéronautiques, Paris, France

1 Instituto Nazionale per Studi de Esperienze di Architettura Navale, Rome, Italy

1 Canal de Experienceas Hidrodinamicas, El Pardo, Madrid, Spain

1 Institut de Recherches de la Construction Navale, Paris, France

1 Nederlandsh Scheepsbouwkundig Proefstation, Haagsteeg, Wageningen, The Netherlands

1 Skipsmodelltanken, Tyholt Trondheim, Norway

1 Statens Skeppsprovningsanstalt, Göteborg, Sweden

1 Hamburg Model Basin, Hamburg, Germany

9 ALUSNA, London, England

1 BSRA, London, England

9 BJSM(NS)

3 CJS

NAVY DPPO PRNC WASH D C